Title

Direct CD137 costimulation of CD8 T cells promotes retention and innate-like function within nascent atherogenic foci

Authors

Maria M. Xu,[1] Antoine Ménoret,[1,2] Sarah-Anne E. Nicholas,[3] Sebastian Günther,[4] Eric J. Sundberg,[4,5,6] Beiyan Zhou,[1] Annabelle Rodriguez,[3] Patrick A. Murphy,[3*] and Anthony T. Vella[1*]

* = co-corresponding authorship

Author Contributions

M.M.X., P.A.M., and A.T.V. conceived and designed the research studies. M.M.X. analyzed data, prepared figures, and drafted the manuscript under editing and revision supervision of A.T.V. and P.A.M. Experiments were performed by M.M.X., P.A.M., A.M., and S.-A.E.N. Reagents were provided by E.J.S. and S.G. and A.R. and B.Z. provided conceptual feedback critical to the development of the manuscript. E.J.S., S.G., A.R., and B.S. helped interpret results of experiments. M.M.X., A.M., S.-A.E.N, S.G., E.J.S., B.Z., A.R., P.A.M., and A.T.V. approved the final version of manuscript.

Affiliations

[1]Department of Immunology, UConn Health School of Medicine, Farmington, CT
[2]Institute for Systems Genomics, UConn Health School of Medicine, Farmington, CT
[3]Center for Vascular Biology, School of Medicine UConn Health, Farmington, CT
[4]Institute of Human Virology, University of Maryland School of Medicine, Baltimore, MD
[5]Department of Medicine, University of Maryland School of Medicine, Baltimore, MD
[6]Department of Microbiology and Immunology, University of Maryland School of Medicine, Baltimore, MD

Running Title

Effector CD8 T cells seed atherogenic foci

Address for Correspondence

A.T.Vella
Department of Immunology
School of Medicine
UConn Health
263 Farmington Ave
Farmington, CT 06030
vella@uchc.edu
phone: (860) 679-4364
fax: (860) 679-8130

ABSTRACT

Effector CD8 T cells infiltrate atherosclerotic lesions and are correlated with cardiovascular events, but the mechanisms regulating their recruitment and retention are not well-understood. CD137 (4-1BB) is a costimulatory receptor induced on immune cells and expressed at sites of human atherosclerotic plaque. Genetic variants associated with decreased CD137 expression correlate with carotid-intimal thickness and its deficiency in animal models attenuates atherosclerosis. These effects have been attributed in part to endothelial responses to low and disturbed flow (LDF), but CD137 also generates robust effector CD8 T cells as a costimulatory signal. Thus, we asked whether CD8 T cell-specific CD137 stimulation contributes to their infiltration, retention, and IFNγ-production in early atherogenesis. We tested this through adoptive transfer of CD8 T cells into recipient C57BL/6J mice that were then antigen-primed and CD137-costimulated. We analyzed atherogenic LDF-vessels in normolipidemic and PCSK9-mediated hyperlipidemic models and utilized a digestion protocol that allowed for lesional T cell characterization via flow cytometry and *in vitro* stimulation. We found that CD137 activation, specifically of effector CD8 T cells, triggers their intimal infiltration into LDF-vessels and promotes a persistent innate-like pro-inflammatory program. Residence of $CD137^+$ effector CD8 T cells further promoted infiltration of endogenous CD8 T cells with IFNγ-producing potential, while CD137-deficient CD8 T cells exhibited impaired vessel infiltration, minimal IFNγ-production, and reduced infiltration of endogenous CD8 T cells. Our studies thus provide novel insight into how CD137 costimulation of effector T cells, independent of plaque-antigen recognition, instigates their retention and promotes innate-like responses from immune infiltrates within atherogenic foci.

Keywords: Atherosclerosis, Inflammation, CD137, CD8 T cell, IFNγ

NEW & NOTEWORTHY

Our studies identify CD137 costimulation as a stimulus for effector CD8 T cell infiltration and persistence within atherogenic foci, regardless of atherosclerotic-antigen recognition. These costimulated effector cells, which are generated in pathologic states such as viral infection and autoimmunity, have innate-like pro-inflammatory programs in circulation and within the atherosclerotic microenvironment, providing mechanistic context for clinical correlations of cardiovascular morbidity with increased CD8 T cell infiltration and markers of activation in the absence of established antigen-specificity.

Atherosclerosis is a complex disease laced by not only passive lipid accumulation, but also immune cell recruitment and endothelial cell (EC) activation (22, 56). Low and disturbed flow (LDF) is an established activator of ECs, instigating transcriptional programs that facilitate pathologic infiltration of T cells, macrophages, dendritic cells, and others through upregulation of adhesion receptors, cytokines, and chemokines (16, 18, 37). Once resident within the vascular wall, these foci of immune infiltrates contribute to the development of atherosclerotic lesions at sites of LDF: geometric curvatures such as the aortic arch, branch points along the abdominal aorta, and the junction of the right subclavian and brachiocephalic arteries (9, 22). Accelerated by systemic inflammation, including activation of the adaptive immune system, these lesions develop into plaques that are prone to rupture and endothelial erosion, leading to the adverse health events associated with atherosclerosis (24).

Though CD8 T cells are among the first to infiltrate atherogenic foci (22) and their frequency within human plaques has been correlated with intima-media carotid thickness and rate of cardiovascular events (31, 71), their role in the pathologic progression of atherosclerosis is not well-understood. This is in part because they are not as abundant within developed atherosclerotic plaques as macrophages, but also because their characterization has been largely limited to histoanalyses due to lack of dedicated isolation protocols that allow for single-cell characterization of lesion-infiltrated cells (54). Nonetheless, immunostaining of a human aortic biobank has revealed that CD8 T cells accumulate within plaque intima during pre-thrombotic development of pathologic fibroatheromas and that CD8 T cells are the dominant $CD3^+$ population within early fibroatheromas, outnumbering $CD4^+$ T cells in a ratio of 5:1 (64). Additionally, histoanalyses of human atherosclerotic plaque suggest that lesional T cells sustain an activated phenotype based on their expression of surface molecules and proximal location to IFNγ cytokine staining (23, 29, 61). In patients with chronic infections, such as Human Immunodeficiency Virus or Cytomegalovirus, markers of activated CD8 T cells in circulation are also associated with increased plaque severity (4, 26, 39, 63). Further, increased circulation of activated T cells, as in autoimmunity, is an independent risk factor for cardiovascular events (58). Patients with type 1 diabetes (10), psoriasis (17), inflammatory bowel disease (49), multiple sclerosis (6), and systemic lupus erythematous (12) face accelerated pathologic progression of atherosclerosis and increased rates of cardiovascular morbidity.

Within hyperlipidemic mouse models, CD8 T cells similarly infiltrate plaques at early stages of atherosclerosis (2, 32) and the pathologic role of CD8 T cells in the inflammatory cascade has been established through antibody depletion (8, 35). In mice, the lesional area of individual atherogenic foci and number of infiltrated T cells is small, but protocols have recently been developed to address the need for flow cytometric characterization of murine infiltrated cells (19). These studies have focused on assessing the infiltration dynamics of leukocytes and T cell populations as a whole, and thus subtype-specific analyses warrant further investigation (15). In the current absence of phenotypic characterization of specific T cell subtypes from atherosclerotic lesions, it has been conventionally believed that they maintain a classical antigen-dependent effector function. While plaque-specific byproducts may have significant roles in the activation and expansion of infiltrated T cells, the heterogeneity of T cell receptors (TCRs) within plaque is suggestive of a broader T cell infiltrate than one resulting from antigen-dependent clonal expansion alone (47, 61). In antiviral immunity, CD8 T cells are responsive to cytokine stimulation, secreting pro-inflammatory cytokines as a “bystander effect” in the absence of cognate antigen restimulation (3, 11). These cells are often identified by their expression of non-conventional T cell surface molecules, including those classically associated with natural killer cells (e.g. CD161) or dendritic cells (e.g. CD11c), and are generated after antigen priming, as in viral infections (30, 34). Costimulated effector CD8 T cells similarly produce IFNγ in response to cytokine signals (62) and thus, it is plausible that peripherally-

activated CD8 T cells infiltrate atherosclerotic plaque and mediate its pathologic progression through “innate-like” production of cytokines such as IFNγ (46, 51).

CD137 (4-1BB) is a tumor necrosis factor costimulatory receptor induced on a range of immune cells, but also expressed at sites of human atherosclerotic plaque and genetically correlated with atherosclerotic disease (48, 59). CD137 was first identified as an inducible T cell gene expressed upon antigen activation (72) and now, CD137-agonistic regimens are being employed to generate durable effector CD8 T cell responses against certain cancers (40). Within human plaque, CD137 co-localizes with both ECs and CD8 T cells (48). Additionally, soluble CD137, which is released by leukocytes after activation and is elevated in autoimmunity (42, 57), correlates with increased risk of cardiovascular events in patients with acute coronary syndrome (73, 74). In hyperlipidemic mouse models, global CD137 deficiency decreases plaque lesion size and diminishes monocyte/macrophage infiltration (27), while agonistic CD137 activation facilitates plaque development (38, 60). Bone marrow transplant experiments have hinted at a pro-atherogenic role for CD137 in circulating blood cells (27), but the specific circulating populations responsible have not yet been defined.

Previous studies have laid the framework for CD137 mediating atherosclerotic pathology, but elucidating the specific cell types that CD137 pathologically affects would provide mechanistic context for why autoimmunity and viral infection confer increased atherosclerotic risk and could also inform long-term risk profiles for patients undergoing CD137-agonistic cancer immunotherapies. Given the dual significance of CD137 activation at sites of atherosclerotic plaque and in activating antigen-primed CD8 T cells into effector cells with inflammatory cytotoxic potential, we wondered how CD137 activation of effector CD8 T cells specifically impacts their pathologic infiltrative and inflammatory programs. In particular, we focused on characterizing the inflammatory phenotype of lesional T cells and questioned whether, as we had observed in other contexts (62), CD137 activation generates TCR-independent programs. To test the effect of CD137 specifically on effector CD8 T cells, we used adoptive transfer of congenically marked WT or CD137-deficient CD8 T cells specific for non-plaque antigen. Immunization and CD137 costimulation of the host mouse allowed us to then isolate the effect of CD137-costimulation on effector CD8 T cells from previously reported pro-inflammatory effects of the host vasculature. Through this adoptive transfer technique and the application of a new digestion protocol for isolating lesional T cells, we were able to study how CD137 costimulation triggers effector CD8 T cells to infiltrate, persist, and sustain innate-like inflammatory programs within LDF-mediated atherogenic foci.

157 ***Mice.***

158 All animal studies were performed in accordance with UConn Health (Farmington, CT)
159 Institutional Animal Care and Use Committee regulations. CD45.2 C57BL/6J (WT) mice were
160 purchased from The Jackson Laboratory (Bar Harbor, ME). Ova (SIINFEKL$^{257-264}$)-specific OT-I
161 TCR transgenic, recombination activating 1-deficient (*Rag1*$^{-/-}$) mice that were WT or CD137$^{-/-}$
162 on C57BL/6J CD45.1 or CD45.1/2 Het background were bred in-house. All mice were
163 maintained in the UConn Health Animal Facility in accordance with National Institutes of Health
164 guidelines. All mice used in these studies were between 1.5 and 8 months.

165 ***Hyperlipidemia.***

166 Mice received 100 µL intraperitoneal injection of 1x10^{11} viral particles of AAV8-encoding mutant
167 PCSK9 (pAAV/D377Y-mPCSK9) produced at the Gene Transfer Vector Core (Grousbeck Gene
168 Therapy Center; Harvard Medical School). Considering the differential response of male vs.
169 female mice to viral production (66), only male mice were used for hyperlipidemia studies to
170 achieve a consistent response to virally produced mPCSK9 protein. Between 1 and 5 d after
171 AAV injection, mice were placed on Clinton/Cybulsky High Fat Rodent Diet with Regular Casein
172 and 1.25% added Cholesterol (Research Diets Inc D12108C) (HFD). To measure cholesterol
173 levels, blood was collected from the right ventricle into lithium heparinized tubes (BD
174 Biosciences 365965) and centrifuged at 5,000 g for 10 min to obtain serum. Samples were
175 stored at -80ºC and analyzed by Total Cholesterol Assay Kit (Cell Biolabs, INC Cat: STA-384).

176 ***Surgical induction of LDF.***

177 Partial carotid artery ligation (PCAL) (45) was performed as previously described (43, 44). In
178 brief, mice were anesthetized with isoflurane and the left external carotid, internal carotid, and
179 occipital artery were ligated with 9-0 Ethilon suture (Ethicon, US stock 2813G). Sham operation
180 controls were conducted in separate mice where the left carotid branches were encircled with
181 suture as in PCAL, but vessels were not ligated. High resolution Doppler ultrasound (Vevo
182 2100) was performed one wk after ligations to confirm vessel patency and reduction in flow.

183 ***Adoptive Transfer and Immunizations.***

184 Naïve splenic OT-I cells (5x10^5 viable CD8$^+$ Vα2$^+$ Vβ5$^+$ CD45.1$^+$ CD44^{low}) were intravenously
185 transferred into WT recipients. Recipient mice were injected intraperitoneal with 100 µg
186 SIINFEKL$^{257-264}$ peptide (InvivoGen, San Diego, CA) + 100 µg of rat IgG control or agonist anti-
187 CD137 (Clone 3H3 mAb, Bio X Cell) 4-24 h after adoptive transfer.

188 ***Vessel Harvests.***

189 Vessels were flushed with phosphate buffered saline (PBS) through the left ventricle and out the
190 right atrium, then dissected free of adventitial tissue, minced with scissors into 1.5 mL
191 Eppendorfs, and incubated for 1 h at 37ºC with gentle rotation (20 rpm) in balanced salt solution
192 (BSS) media containing: 150 U/mL Collagenase type IV (Sigma-Aldrich C5138), 60 U/mL
193 DNase I (Sigma-Aldrich), 1 µM $MgCl_2$ (Sigma Aldrich), 1 µM $CaCl_2$ (Sigma-Aldrich), and 5% fetal
194 bovine serum (FBS). Digested tissues were crushed through 35 µm cell-strainer caps (BD
195 Biosciences) and quenched with 5 mL cold BSS + 10% FBS in round-bottom tubes.
196 Supernatant was removed after a 5 min 320 g centrifuge and the cell pellet was re-suspended
197 and quantified using Z1 particle counter (Beckman Coulter).

198 ***in vitro stimulations.***

199 All stimulations were conducted at 37ºC and 5% CO_2 in 200 µL complete tumor medium
200 consisting of modified Eagle's medium with 5% FBS, amino acids, salts and antibiotics in 96-
201 well plates. Carotid and aortic arch vessels were seeded at 7.5x10^3 cells/well; blood and spleen
202 cells at 1.5x10^4 cells/well. Stimulations were with Phorbol 12-myristate 13-acetate (PMA) (50
203 ng/ml Calbiochem, Darmstadt, Germany) + ionomycin (1 µg/ml Invitrogen), murine cytokines

IL-2 (5 ng/mL) and N-terminally processed IL-36 (1 μg/mL) (produced according to previous protocols(21) and R&D Systems), or SIINFEKL peptide (1 ng/mL, InvivoGen) for 60-65 h. Secreted IFNγ was analyzed in culture supernatants by ELISA (R&D Systems, Minneapolis, MN).

Flow Cytometry.

Surface staining: naïve OT-I splenocytes for adoptive transfer were identified as (catalog/clone): LIVE/DEAD Fixable Blue Dead$^-$ (ThermoFischer L23105), CD8$^+$ (BD Biosciences 558106/53-6.7), CD4$^-$ (Tonbo 60-0042/RM4-5), B220$^-$ (BD Bioscience 553093/RA3-6B2), CD45.1$^+$ (eBioscience 17-0453-82/A20), CD45.2 (Invitrogen 11-0454-81/104), Vα2$^+$ (eBioscience 46-5812-80/B20.1), Vβ5$^+$ (BD Bioscience 553190/MR9-4), and CD44^{lo} (Tonbo 80-0441/IM7). Analysis of vessel-infiltrated cells was conducted using: LIVE/DEAD Fixable, CD4 (Invitrogen), CD45.1 (eBioscience), CD45.2 (Invitrogen), Vα2 (eBioscience), Vβ5$^+$ (BD Bioscience), B220 (BD Bioscience), CD3 (BD Bioscience 562600/145-2011), CD8 (Invitrogen MA5-17595/CT-CD8a), Streptavidin (BD Pharmingen 554063), and CD11c (Tonbo 80-0032/17A2). LSR Aria IIa (BD Biosciences) was used for acquisition. Viable cell gate is representative of a size gate, single cell gate, and viability gate.

For intracellular staining, cells were incubated for the last 5 h in the presence of GolgiStop (BD Biosciences), surface stained, permeabilized and fixed via FoxP3 fixation kit (eBioscience), and stained at 4ºC overnight with IFNγ (BD Pharmingen 554412/XMG1.2). Acquisition was performed by MACSQuant (Miltenyi Biotec). All flow cytometry data was analyzed with FlowJo (Tree Star, Ashland, OR).

Immunohistofluoresence.

Vessels were flushed *in situ* with PBS before resection, then fixed in 4% buffered paraformaldehyde overnight at 4ºC, dehydrated in 30% wt/vol sucrose overnight, then snap-frozen in OCT and stored at -80ºC. Specimens were sectioned at 10 μm and fixed for 2-10 min in ice-cold acetone before staining at room temperature. Slides were air dried before PBS rehydration and blocked for 1 h with 0.01% Triton X-100 (BioRad), 2.5% wt/vol bovine serum albumin (Sigma-Aldrich) and 2.5% goat serum (Invitrogen). Sections were stained with CD31 (Biolegend 102502/Mec13.3 at 1 μg/mL) and CD45.1 (Biolegend 110720/A20 at 1 μg/mL) for 2 h, followed by goat anti-rat IgG Alexa Fluor 594 (Invitrogen A-11007 at 2 μg/mL) and DAPI staining for 1 h. Fluoromount-G™ (ThermoFischer) was used to mount slides before imaging on Zeiss LSM 800 confocal at 20x and 63x magnification. Image J Cell Counter was used to quantify images taken at 20x with CD45.1 threshold set to 100. DAPI split channel images where thresholded between 90 and 255. Lumen surface was defined as a CD45.1$^+$ cell in contact with the luminal CD31 EC lining and intimal infiltration as CD45.1$^+$ staining between the EC and medial elastin layers of the vessel wall.

CyTOF.

After PBS-flushed arteries were digested to liberate infiltrated cells, cells isolated from 5 ligated or contralateral control carotid vessels were respectively pooled to obtain sufficient cell number for CyTOF processing. Analyses and labelling were conducted as previously described (41). The pooled samples were analyzed by a mass cytometer (Helios, Fluidigm), data de-barcoded using Fluidigm Debarcoder v1.04, and then merged to create viSNE maps using Matlab (MathWorks, Natick, MA). All antibodies (Supplemental Table 1) were from Fluidigm (South San Francisco, CA).

Statistics.

Unless otherwise indicated, dots represent an individual biologic replicate and summary graphs represent mean ± standard deviation. Analyses were performed with GraphPad Prism V7 (GraphPad Software). For comparisons within groups, we used paired, 2-tailed Student's t-tests

("paired t-test" in text) and for comparisons between groups, we used 2-group, 2-tailed Student's t-tests ("2-group t-test" in text). When there was a noticeable departure from normality, non-parametric tests based on ranks were used (e.g. Figure 5, 8, and S6, which used Mann-Whitney tests for 2-group analyses and Wilcoxon matched-pair tests for paired analyses, as appropriate). *P* values <0.05 were considered statistically significant and are further defined as indicated.

Effector CD8 T cells infiltrate low and disturbed flow-activated endothelium.

To examine pathologic immune infiltration into nascent atherogenic foci, we combined Partial Carotid Artery Ligation (PCAL) with AAV-mPCSK9, surgically inducing LDF within the geometrically straight left carotid in the setting of rapid LDL-receptor deficiency-mediated hyperlipidemia (Figure 1A) (33, 55). PCAL entails ligation of all but one branch of the left carotid, generating LDF throughout the left carotid artery and leaving the contralateral right carotid artery as an internal control subject to its physiologic laminar flow patterns. When combined with high fat diet (HFD), WT C57BL/6J mice develop hyperlipidemia within days that was sustained at an experimental endpoint of 3 wks (Figure 1B). Consistent with previous studies (33), we found that PCAL induces lipid-laden plaque within 4 wks (Figure 1C). This plaque is also cellularized in a LDF-dependent manner (Supplemental Figure S1A). Thus, PCAL induces lipid and cell accumulation at atherogenic foci and serves as an experimental model of nascent, LDF-dependent cell infiltration.

To study the infiltration of peripherally-generated effector CD8 T cells into PCAL-ligated vessels, we transferred TCR-transgenic CD45.1 (OT-I, Ova-specific) cells into recipient WT mice with established mPCSK9-mediated hyperlipidemia (Figure 2A). Activated effector CD8 T cells were generated by immunizing recipient mice with cognate SIINFEKL peptide and costimulatory agonist anti-CD137 mAb 4-24 h after adoptive transfer. When compared to mice that received rat IgG control, increased IFNγ responsiveness of both splenocytes and blood cells to the mitogen PMA + ionomycin 4 days post immunization (dpi) was dependent on prior *in vivo* CD137 costimulation (Figure 2B). Vessel infiltration of transferred and endogenous T cells was analyzed through digest of PBS-flushed arteries and flow cytometry (Figure 2C). A digest protocol was developed to maximize isolation of lymphocytes while also preserving cell viability for not only flow cytometry characterization, but also *in vitro* restimulation experiments (detailed in methods). Consistent with previous reports (48), CD137 costimulation did not significantly affect infiltration of CD4 T cells (Supplemental Figure S1B). Yet, CD137 costimulation significantly increased infiltration of transferred effector CD8 T cells into PCAL-ligated carotids by both percentage of viable cells and total count of transferred CD8 T cells isolated per vessel (Figure 2D). This CD137-mediated infiltration was also observed within regions of physiologic LDF such as the aortic arch (Figure 2E). Parallel to the clinical observation that systemic inflammation predisposes autoimmune patients to atherosclerotic pathology regardless of lipid levels (52, 58), normolipidemic mice fed chow diet and mPCSK9-hyperlipidemic mice on HFD had no obvious difference in effector cell infiltration, by either percentage or total cell count, into physiologic areas of LDF 4 dpi, and cholesterol level in hyperlipidemic mice had no significant correlation with effector cell infiltration into ligated and physiologic LDF foci (Supplemental Figure S2). Thus, effector CD8 T cells accumulate at induced and physiologic sites of LDF independent of cholesterol levels; their distribution *in situ* could reveal parallels with human CD8 T cell plaque-residence.

Localization of effector CD8 T cells was visualized by immunofluorescent staining of carotid artery cross-sections (Figure 3A-B). The EC layer was demarcated by CD31 (platelet endothelial cell adhesion molecule) and transferred CD8 T cells by CD45.1. Total infiltration of transferred CD8 T cells per cross-section was increased upon CD137 costimulation and this was due to increased numbers deep within the intima, not at the abluminal surface (Figure 3C). The underlying medial and adventitial layers were minimally infiltrated by effector CD8 T cells (Supplemental Figure S3), suggesting that the immune-privileged medial status had not been compromised, consistent with early-stage human atherosclerotic lesions (64). Having established that effector CD8 T cells infiltrate neointima at sites of induced and physiologic LDF in a manner similar to human plaque, we sought to gain mechanistic insight into their potential role within atherosclerotic pathology.

Infiltrated effector CD8 T cells have robust inflammatory potential

To test for differences in infiltrative cell phenotype downstream of both surgically-induced and physiologic LDF patterns, we performed cytometry by time of flight (CyTOF) analysis on cells isolated from PCAL-carotids, contralateral control carotids, and physiologic LDF vessels 4 dpi with cognate antigen and CD137 costimulation (Figure 2A). ViSNE maps of PCAL-ligated and control carotid vessels revealed two islands of cells dominated by cells isolated from PCAL-ligated vessels (Supplemental Figure S4). LDF Group 1 appeared to be dominated by endogenous monocytes and a small population of $CD4^+$ T cells, whereas LDF Group 2 was dominated $CD45.1^+$ cells that were largely $CD8^+$, representing the transferred Ova-specific population of effector CD8 T cells. This group also expressed Granzyme B and markers associated with innate-like CD8 T cell responses; the conventional dendritic cell marker CD11c (5, 50, 65) and natural killer cell marker CD161 (13). Thus, not only do effector CD8 T cells infiltrate surgically-induced and physiologic atherogenic foci, but they also express enzymes and surface markers suggestive of responsiveness to non-antigen stimuli.

To assess if the local cytokine environment could potentially play a role in antigen-independent activation of infiltrated effector CD8 T cells, we tested for expression of all pro-inflammatory IL-1 cytokines in the intimal response to LDF (43), as we had previously described effector T cells having innate-like responses to IL-1 cytokines when combined with IL-2 (62), a cytokine found within plaques (14). This revealed LDF-mediated upregulation of IL-36γ and IL-1β (Supplemental Figure S5A). Like other IL-1 cytokines, IL-36 requires N-terminal cleavage for full biologic activity and the associated protease Cathepsin S (1) was similarly upregulated by LDF. IL-1β has a well-studied role in mediating atherosclerosis (53) and IL-36γ a prominent role in psoriasis, but IL-36γ has not yet been studied in atherosclerosis. Thus, informatics analysis (Supplemental Figure S5) suggested a possible role for IL-1β and IL-36γ in mediating antigen-independent CD8 T cell activation within the inflamed intima.

To determine whether IL-1β and/or IL-36γ could elicit innate-like secretion of IFNγ from dual-costimulated effector CD8 T cells as we had previously studied (62), we exposed splenocytes *in vitro* to these cytokines in combination with IL-2. IL-1β, both alone and in combination with IL-2, did not elicit IFNγ production (Supplemental Figure S5C). However, IL-36γ + IL-2 induced a dose-dependent production of IFNγ from both dual-costimulated CD8 T cells and whole splenocytes harvested 4 dpi with SIINFEKL and CD137 mAb (Figure 4A-B). To determine if the intima-infiltrated transferred effector CD8 T cells were similarly capable of responding to cytokines (IL-2 and IL-36γ), we compared *in vitro* IFNγ secretion from cells isolated from LDF regions (surgically-induced and physiologic) with cells isolated from linear carotid arteries as a control. We observed increased IFNγ secretion from cultures of LDF infiltrates, both within the abdominal aorta and PCAL-carotids (Figure 4C-D), while cells isolated from the contralateral control carotids failed to produce detectable amounts of IFNγ. Further, IFNγ secretion trended with number of infiltrated effector CD8 T cells per vessel (Supplemental Figure S5B), suggesting that these are the cells responsible for producing the majority of IFNγ, a concept further defined by intracellular staining studies shown in Figure 8. Having established that peripherally-activated effector CD8 T cells exhibit innate-like pro-inflammatory programs *in situ,* our goal was then to resolve the role of T cell-CD137 signaling in mediating this process.

T cell CD137 expression is critical for robust infiltration of effector CD8 T cells to LDF-activated endothelium

To delineate the requirement for CD137 on CD8 T cells versus other CD137-expressing cells within LDF atherogenic intima, the infiltrative capacity of transferred $CD137^{-/-}$ CD8 T cells was examined in WT recipient mice immunized with cognate SIINFEKL peptide and agonistic anti-CD137 mAb (Figure 5A). T cell CD137 expression was required for robust infiltration into

the aortic arch by both percentage (Figure 5B) and cell count (Figure 5C). Similar trends were observed in the PCAL model of LDF, although statistical significance was not reached (Supplemental Figure S6A). Thus, even when the recipient environment of LDF-activated endothelium is CD137-sufficient (including other T cell subtypes (68), monocytes (36), dendritic cells (69), and natural killer cells (70)), significant infiltration of effector CD8 T cells into neointima requires their own activation through CD137 costimulation. If this infiltration is persistent, these innate-like CD8 T cells could have biologic relevance within atherosclerosis.

Persistence of effector CD8 T cells requires T cell CD137

To test if CD137 expression on transferred CD8 T cells impacted persistence within atherosclerotic plaque, we transferred a 1:1 mixture of WT ($CD45.1^+$) and $CD137^{-/-}$ (CD45.1/45.2 Het) Ova-specific CD8 T cells into WT recipient mice ($CD45.2^+$) that then received cognate SIINFEKL peptide and CD137 costimulation (Figure 6A). The distribution of each congenically marked population within blood and their infiltration into LDF-vessels was assessed through flow cytometry (Supplemental Figure S6B). Between 5 and 11 dpi, the percentage of viable cells (Figure 6B) and cell count (Figure 6C) of transferred CD8 T cells isolated from the Aortic Arch did not significantly change, despite a significant drop in the proportion of transferred, WT Ova-specific CD8 T cells circulating within spleen and blood over the same timecourse (Figure 6C). Accompanying the increased infiltration of WT transferred effector CD8 T cells were endogenous populations of CD8 T cells (Figure 6D). To further assess the persistence of the transferred CD137-costimulated effector CD8 T cells within LDF foci, we used hyperlipidemic PCAL mice (as in Figure 2A) and administered a 1:1 WT and $CD137^{-/-}$ mixture of Ova-specific CD8 T cells. Strikingly, only the infiltration of WT Ova-specific CD8 T cells was preferential to LDF-ligated carotids 17 dpi (Figure 6E). Thus, CD137-costimulated effector T cells persist for weeks within LDF-activated foci independent of plaque-antigen specificity and their infiltration is accompanied by the infiltration of other T cells, perhaps indicative of progressive plaque pathology.

Infiltration of effector CD8 T cells promotes a diverse, pro-inflammatory CD8 T cell infiltrate

Atherosclerosis is a chronic disease in which LDF regions are repetitively exposed to T cells activated by environmental antigen or costimulation signals, exposures which could pathologically seed atherogenic foci with effector CD8 T cells. To assess how T cell CD137 influences the persistence of these infiltrated T cells, WT or $CD137^{-/-}$ Ova-specific CD8 T cells were transferred into hyperlipidemic recipient mice, provided a single injection of cognate SIINFEKL peptide and agonist anti-CD137 mAb, and then analyzed 30 dpi (Figure 7A). At this timepoint, the overt cell expansion induced by antigen-priming and costimulation has subsided in spleen and in circulation (Supplemental Figure S7A). Through both percentage and total cells isolated per vessel, T cell expression of CD137 was necessary for effector CD8 T cell persistence within the aortic arch (Figure 7B). Immunohistofluoresence of another physiologic foci of LDF, the branch point of the right subclavian artery from the brachiocephalic artery, revealed that the transferred CD8 T cell population infiltrates and persists within plaque intima at physiologic sites of LDF-mediated atherogenesis (Figure 7C). Thus, a single, acute activation of CD8 T cells may indeed lead to their chronic persistence within plaque intima, perhaps imprinting an inflammatory signature and progressive plaque phenotype.

We then tested whether these T cells retained inflammatory responses, as we had observed 4 dpi during their phase of acute expansion (Figure 2, 4). Cells isolated from the aortic arch were stimulated *in vitro* with PMA + ionomycin to broadly assess their IFNγ-producing potential. Through both ELISA (Supplemental Figure S7B) and intracellular cytokine staining (Figure 8B), it was confirmed that expression of CD137 on transferred CD8 T cells endows

developing atherogenic foci with inflammatory cell infiltrates. To define these pro-inflammatory plaque-resident populations, we analyzed surface expression of the IFNγ$^+$ population from mice receiving WT CD8 T cells and found that the majority were transferred Ova-specific cells (CD45.1$^+$), suggesting that even 30 dpi, an inflammatory program is sustained (Figure 8B). Parallel to this persistence of transferred effector CD8 T cells was the infiltration of endogenous (CD45.2$^+$) CD8 T cells, which composed a substantial compartment of the PMA + ionomycin inflammatory response. This endogenous CD8 population was composed of both "Other" (non-Vα2Vβ5) and endogenous Vα2$^+$Vβ5$^+$ CD8 T cells, which are largely Ova-specific (25) (Figure 8C). Notably, infiltration of non-Vα2Vβ5 CD8 T cells was significantly higher in mice that received transfer of WT, CD137$^+$ Ova-specific CD8 T cells (Figure 8C). Infiltration of CD4 T cells into the aortic arch was not significantly affected by CD137 expression of the transferred CD8 T cells (Supplemental Figure S7C). Thus, not only is T cell CD137 requisite for effector CD8 T cell persistence within LDF vessels, but it also promotes the infiltration of additional CD8 T cells that have pro-inflammatory IFNγ-producing programs.

To test if the immune infiltrate directed by intimal infiltration of WT CD137$^+$ effector CD8 T cells into LDF foci maintained an innate-like inflammatory program, we assessed their surface expression and functional capacity to respond to cognate antigen or instead, cytokines. CD11c expression was analyzed, as it was a marker initially identified to be expressed 4 dpi (Supplemental Figure S4). Not only did the transferred CD8 T cells have significantly higher CD11c MFI than all other T cell subtypes isolated from the Aortic Arch (Figure 8D), but they also had preserved innate-like IFNγ responses to the cytokines IL-2 and IL-36, as supported by intracellular cytokine staining (Figure 8E). While the percentage of IFNγ$^+$ T cells was not substantially different through this assay, which is limited in time course by the toxicity of the agent used to prevent secretion of IFNγ, analysis of cell culture supernatant for cumulative IFNγ secretion was significantly higher in mice that received transfer of WT Ova-specific CD8 T cells (Figure 8F). Further, this innate-like production of IFNγ was stronger than cognate antigen-restimulation, while splenocytes from the same mice had a stronger response to SIINFEKL peptide re-stimulation than to the cytokines (Supplemental Figure S7D). Mice that received CD137$^{-/-}$ Ova-specific CD8 T cells did not have cytokine-mediated or antigen-restimulation responses significant over media control. Thus, CD137 activation of effector CD8 T cells promotes their infiltration into vascular sites of LDF, and once seeded within atherogenic foci, they are responsive to the inflammatory cytokine environment where their chronic intimal persistence facilitates subsequent infiltration of other CD8 T cells.

Using *in vivo* mouse models of surgically-induced and physiologic LDF, we show that activation of CD137 on CD8 T cells promotes their neointimal infiltration within developing atherogenic foci, independent of plaque-specific antigen recognition. Once resident, these CD137-stimulated effector CD8 T cells are retained and express markers and phenotypes akin to innate-like cells. Mechanistically, we show that both IL-36γ and the enzyme required for its activating cleavage, Cathepsin S, are upregulated at atherogenic foci. Further, the combination of IL-36γ with IL-2, a cytokine native to neointimal environments, is sufficient to induce innate-like cytokine production from plaque-derived CD8 T-cells *in vitro*. Presence of these innate-like CD8 T cells in the atherogenic intima promotes infiltration of other endogenous CD8 T cells, thereby altering plaque immune cell composition. Thus, through phenotypic and *in vitro* characterization of plaque-lesional T cells, our data support a model in which generation of effector CD8 T cells in circulation, perhaps physiologically induced by systemic viral infection or autoimmunity, drives their infiltration into nascent atherogenic intima where they persist, secrete pro-inflammatory cytokines, and orchestrate additional recruitment of immune cells into nascent atherogenic foci (Figure 9).

Our studies shed light on the complicated role of CD137 in both atherosclerotic plaque development and activation of multiple immune cell types by specifically defining the effects of CD137 on effector CD8 T cells. The significance of delineating this cell type-specific response is reinforced by the apparently contradictory observation that CD137-deficiency in animal models leads to reduced atherogenesis, while a human genetic SNP linked with decreased CD137 mRNA is associated with increased intimal medial thickness (59). Through comparisons of CD137 mAb administration versus rat IgG control (Figure 2-3) followed by adoptive transfer of WT and CD137-deficient Ova-specific CD8 T cells (Figures 5-8), our studies establish CD137 costimulation of effector CD8 T cells as pathologic in promoting their infiltration and retention within atherogenic foci in mice. In light of the emergence of CD137-agonistic cancer immunotherapies (40), understanding how CD137 activation impacts the progression of atherosclerosis, perhaps through the pathologic seeding of CD8 T cells and survival advantage within the plaque microenvironment, is of great clinical importance. Other costimulatory members of the tumor necrosis family have been linked to atherosclerosis(20) and it would be interesting to examine if CD134 (OX40), LIGHT, and CD70 have similar means of orchestrating additional inflammatory infiltrate, or if CD137 is unique in its specificity for promoting effector CD8 T cell infiltration into atherogenic foci.

Plaque-specific antigens have clear significance in CD4 T cell-mediated atherosclerotic pathology (22), but our data supports a model in which circulation of effector CD8 T cells, even if generated peripheral to the atherosclerotic lesion, leads to plaque infiltration from the vessel lumen that is independent of classic lesional antigen recognition. Shortly after direct CD137 costimulation of Ova-specific CD8 effector T cells, we observed their accumulation within the neointima of atherogenic foci (Figure 3). This infiltration was persistent and their intimal localization could be visualized even 30 dpi (Figure 7). Recent single-cell immune-profiling of atherosclerotic lesions has reported not only that T cells are a significant component of atherosclerotic lesions, but that they also have surprisingly high sub-lineage heterogeneity, equivalent in cluster number to those identified within the spleen (71). Whether antigen-independent infiltration of atherogenic foci is limited to effector CD8 T cells, or is applicable to all T cell subsets, has not, to our knowledge been explored. However, we consistently observed no substantial effect of CD137 costimulation on the infiltration of endogenous CD4 T cells into atherosclerotic lesions. Thus, our data suggest that CD137 costimulation, especially when layered with antigen activation, is pathologic in seeding atherogenic foci with effector CD8 T cells, which has implications in autoimmunity and chronic viral infection, where local presentation of CD137-ligand could be constantly generating autoreactive effector CD8 T cells

that are infiltrative and supportive of an intimal niche that is permissive to further inflammatory immune cell infiltration.

Human histoanalyses have identified a clear CD8 infiltrate “footprint” which precedes the formation of advanced and unstable plaque (64), but how these intimal-localized CD8 T cells contribute to destabilizing inflammation is not fully understood. Although lipid byproducts and heat shock proteins have been described as auto-antigens local to the atherosclerotic plaque that are capable of generating effector T cells responses, our prior work with effector T cells highlights other mechanisms of activation (62). Through stimulation of vessel-infiltrated cells with the plaque cytokine IL-36, we show that innate-like responses may be induced by simple proximity to intimal cells upregulating this potent cytokine within LDF-exposed regions of the vasculature (Figure 4, 8). IL-36 is a member of the pro-inflammatory IL-1 family of cytokines and has, only recently, been identified as expressed by ECs in inflamed vasculature (67) and now by LDF-activated atherogenic intima (Supplemental Figure S5A). IL-1β blockade shows therapeutic promise in patients with previous myocardial infarction (53), but IL-36 has distinct signaling mechanisms (21) and our studies suggest that IL-36 is unique amongst the IL-1 family in that it is upregulated by atherogenic intima and is capable of activating innate-like inflammatory programs from plaque-resident CD8 T cells. These responses, which include IFNγ production, are elicited regardless of plaque TCR specificity and may further promote infiltration of other inflammatory cells into nascent atherogenic foci. IL-36 is additionally upregulated in several autoimmune diseases with increased cardiovascular morbidity (7, 28), suggesting that innate-like stimulation of intimal CD8 T cells may indeed have mechanistic contributions to the destabilizing progression of fatty streaks to pathologic plaque.

In conclusion, we show that CD137 stimulation of effector CD8 T cells drives their infiltration specifically into regions of LDF, where they are capable of responding to cytokines within the intimal environment and exhibiting innate-like phenotypes that further promote the recruitment of other CD8 T cells into atherogenic foci. These antigen-independent responses may form the basis for yet unexplored, but more direct mechanisms of pathologic communication with the well-studied cells of the innate immune system. They also suggest that the generation of CD8 effector T cells through a variety of systemic stimuli could drive acute seeding and long-lasting retention of these cells within atherosclerotic plaque, one of the earliest immunologic signatures of unstable plaque progression.

Acknowledgements

We are grateful for the technical support of Brent Heineman *B.A.* (Center for Vascular Biology) who ran the cholesterol measurement assays. We also would like to thank the Institute for Systems Genomics at UConn Health and JAX, Farmington, CT for providing help with the CyTOF studies. Present address for Sebastian Gunther is Deutsches Elektronen-Synchrotron DESY, Hamburg, Germany.

Grants

The work was supported in part by American Heart Association Clinical Health Profession Grant to MMX (Association Wide 17CPRE33660241), the Boehringer Ingelheim Endowed Chair in Immunology, UCONN Health School of Medicine, Farmington, CT to ATV, the National Institutes of Health grant to PAM (R00-HL125727) and AR (5R01HL131862-02), and the Linda and David Roth Chair of Cardiovascular Research to AR.

Disclosures

AR is the founder of Lipid Genomics and A.R. and M.M.X. hold issued patents, but none are related to the topic of this paper.

REFERENCES

1. **Ainscough JS, Macleod T, McGonagle D, Brakefield R, Baron JM, Alase A, Wittmann M, and Stacey M**. Cathepsin S is the major activator of the psoriasis-associated proinflammatory cytokine IL-36gamma. *Proc Natl Acad Sci U S A* 114: E2748-E2757, 2017.
2. **Alberts-Grill N, Rezvan A, Son DJ, Qiu H, Kim CW, Kemp ML, Weyand CM, and Jo H**. Dynamic immune cell accumulation during flow-induced atherogenesis in mouse carotid artery: an expanded flow cytometry method. *Arterioscler Thromb Vasc Biol* 32: 623-632, 2012.
3. **Berg RE, Crossley E, Murray S, and Forman J**. Memory CD8+ T cells provide innate immune protection against Listeria monocytogenes in the absence of cognate antigen. *J Exp Med* 198: 1583-1593, 2003.
4. **Betjes MG, Litjens NH, and Zietse R**. Seropositivity for cytomegalovirus in patients with end-stage renal disease is strongly associated with atherosclerotic disease. *Nephrol Dial Transplant* 22: 3298-3303, 2007.
5. **Beyer M, Wang H, Peters N, Doths S, Koerner-Rettberg C, Openshaw PJ, and Schwarze J**. The beta2 integrin CD11c distinguishes a subset of cytotoxic pulmonary T cells with potent antiviral effects in vitro and in vivo. *Respir Res* 6: 70, 2005.
6. **Bronnum-Hansen H, Koch-Henriksen N, and Stenager E**. Trends in survival and cause of death in Danish patients with multiple sclerosis. *Brain* 127: 844-850, 2004.
7. **Chu M, Wong CK, Cai Z, Dong J, Jiao D, Kam NW, Lam CW, and Tam LS**. Elevated Expression and Pro-Inflammatory Activity of IL-36 in Patients with Systemic Lupus Erythematosus. *Molecules* 20: 19588-19604, 2015.
8. **Cochain C, Koch M, Chaudhari SM, Busch M, Pelisek J, Boon L, and Zernecke A**. CD8+ T Cells Regulate Monopoiesis and Circulating Ly6C-high Monocyte Levels in Atherosclerosis in Mice. *Circ Res* 117: 244-253, 2015.
9. **Combadiere C, Potteaux S, Rodero M, Simon T, Pezard A, Esposito B, Merval R, Proudfoot A, Tedgui A, and Mallat Z**. Combined inhibition of CCL2, CX3CR1, and CCR5 abrogates Ly6C(hi) and Ly6C(lo) monocytosis and almost abolishes atherosclerosis in hypercholesterolemic mice. *Circulation* 117: 1649-1657, 2008.
10. **de Ferranti SD, de Boer IH, Fonseca V, Fox CS, Golden SH, Lavie CJ, Magge SN, Marx N, McGuire DK, Orchard TJ, Zinman B, and Eckel RH**. Type 1 diabetes mellitus and cardiovascular disease: a scientific statement from the American Heart Association and American Diabetes Association. *Circulation* 130: 1110-1130, 2014.
11. **Ehl S, Hombach J, Aichele P, Hengartner H, and Zinkernagel RM**. Bystander activation of cytotoxic T cells: studies on the mechanism and evaluation of in vivo significance in a transgenic mouse model. *J Exp Med* 185: 1241-1251, 1997.
12. **Esdaile JM, Abrahamowicz M, Grodzicky T, Li Y, Panaritis C, du Berger R, Cote R, Grover SA, Fortin PR, Clarke AE, and Senecal JL**. Traditional Framingham risk factors fail to fully account for accelerated atherosclerosis in systemic lupus erythematosus. *Arthritis Rheum* 44: 2331-2337, 2001.
13. **Fergusson JR, Smith KE, Fleming VM, Rajoriya N, Newell EW, Simmons R, Marchi E, Bjorkander S, Kang YH, Swadling L, Kurioka A, Sahgal N, Lockstone H, Baban D, Freeman GJ, Sverremark-Ekstrom E, Davis MM, Davenport MP, Venturi V, Ussher JE, Willberg CB, and Klenerman P**. CD161 defines a transcriptional and functional phenotype across distinct human T cell lineages. *Cell Rep* 9: 1075-1088, 2014.
14. **Frostegard J, Ulfgren AK, Nyberg P, Hedin U, Swedenborg J, Andersson U, and Hansson GK**. Cytokine expression in advanced human atherosclerotic plaques: dominance of pro-inflammatory (Th1) and macrophage-stimulating cytokines. *Atherosclerosis* 145: 33-43, 1999.
15. **Galkina E, Kadl A, Sanders J, Varughese D, Sarembock IJ, and Ley K**. Lymphocyte recruitment into the aortic wall before and during development of atherosclerosis is partially L-selectin dependent. *J Exp Med* 203: 1273-1282, 2006.

16. **Galkina E, and Ley K**. Immune and inflammatory mechanisms of atherosclerosis (*). *Annu Rev Immunol* 27: 165-197, 2009.
17. **Gelfand JM, Neimann AL, Shin DB, Wang X, Margolis DJ, and Troxel AB**. Risk of myocardial infarction in patients with psoriasis. *JAMA* 296: 1735-1741, 2006.
18. **Gimbrone MA, Jr., and Garcia-Cardena G**. Endothelial Cell Dysfunction and the Pathobiology of Atherosclerosis. *Circ Res* 118: 620-636, 2016.
19. **Gjurich BN, Taghavie-Moghadam PL, and Galkina EV**. Flow Cytometric Analysis of Immune Cells Within Murine Aorta. *Methods Mol Biol* 1339: 161-175, 2015.
20. **Gotsman I, Sharpe AH, and Lichtman AH**. T-cell costimulation and coinhibition in atherosclerosis. *Circ Res* 103: 1220-1231, 2008.
21. **Gunther S, and Sundberg EJ**. Molecular determinants of agonist and antagonist signaling through the IL-36 receptor. *J Immunol* 193: 921-930, 2014.
22. **Hansson GK, and Hermansson A**. The immune system in atherosclerosis. *Nat Immunol* 12: 204-212, 2011.
23. **Hansson GK, Holm J, and Jonasson L**. Detection of activated T lymphocytes in the human atherosclerotic plaque. *Am J Pathol* 135: 169-175, 1989.
24. **Hansson GK, Libby P, and Tabas I**. Inflammation and plaque vulnerability. *J Intern Med* 278: 483-493, 2015.
25. **Hogquist KA, Jameson SC, Heath WR, Howard JL, Bevan MJ, and Carbone FR**. T cell receptor antagonist peptides induce positive selection. *Cell* 76: 17-27, 1994.
26. **Hsue PY, Hunt PW, Sinclair E, Bredt B, Franklin A, Killian M, Hoh R, Martin JN, McCune JM, Waters DD, and Deeks SG**. Increased carotid intima-media thickness in HIV patients is associated with increased cytomegalovirus-specific T-cell responses. *AIDS* 20: 2275-2283, 2006.
27. **Jeon HJ, Choi JH, Jung IH, Park JG, Lee MR, Lee MN, Kim B, Yoo JY, Jeong SJ, Kim DY, Park JE, Park HY, Kwack K, Choi BK, Kwon BS, and Oh GT**. CD137 (4-1BB) deficiency reduces atherosclerosis in hyperlipidemic mice. *Circulation* 121: 1124-1133, 2010.
28. **Johnston A, Xing X, Wolterink L, Barnes DH, Yin Z, Reingold L, Kahlenberg JM, Harms PW, and Gudjonsson JE**. IL-1 and IL-36 are dominant cytokines in generalized pustular psoriasis. *J Allergy Clin Immunol* 2016.
29. **Jonasson L, Holm J, Skalli O, Bondjers G, and Hansson GK**. Regional accumulations of T cells, macrophages, and smooth muscle cells in the human atherosclerotic plaque. *Arteriosclerosis* 6: 131-138, 1986.
30. **Kim YH, Seo SK, Choi BK, Kang WJ, Kim CH, Lee SK, and Kwon BS**. 4-1BB costimulation enhances HSV-1-specific CD8+ T cell responses by the induction of CD11c+CD8+ T cells. *Cell Immunol* 238: 76-86, 2005.
31. **Kolbus D, Ljungcrantz I, Andersson L, Hedblad B, Fredrikson GN, Bjorkbacka H, and Nilsson J**. Association between CD8+ T-cell subsets and cardiovascular disease. *J Intern Med* 274: 41-51, 2013.
32. **Kolbus D, Ramos OH, Berg KE, Persson J, Wigren M, Bjorkbacka H, Fredrikson GN, and Nilsson J**. CD8+ T cell activation predominate early immune responses to hypercholesterolemia in Apoe(-)(/)(-) mice. *BMC Immunol* 11: 58, 2010.
33. **Kumar S, Kang DW, Rezvan A, and Jo H**. Accelerated atherosclerosis development in C57Bl6 mice by overexpressing AAV-mediated PCSK9 and partial carotid ligation. *Lab Invest* 97: 935-945, 2017.
34. **Kurioka A, Klenerman P, and Willberg CB**. Innate-like CD8+ T-cells and NK cells: converging functions and phenotypes. *Immunology* 2018.
35. **Kyaw T, Winship A, Tay C, Kanellakis P, Hosseini H, Cao A, Li P, Tipping P, Bobik A, and Toh BH**. Cytotoxic and proinflammatory CD8+ T lymphocytes promote development of vulnerable atherosclerotic plaques in apoE-deficient mice. *Circulation* 127: 1028-1039, 2013.

36. **Langstein J, and Schwarz H**. Identification of CD137 as a potent monocyte survival factor. *J Leukoc Biol* 65: 829-833, 1999.

37. **Ley K, Laudanna C, Cybulsky MI, and Nourshargh S**. Getting to the site of inflammation: the leukocyte adhesion cascade updated. *Nat Rev Immunol* 7: 678-689, 2007.

38. **Li Y, Yan J, Wu C, Wang Z, Yuan W, and Wang D**. CD137-CD137L interaction regulates atherosclerosis via cyclophilin A in apolipoprotein E-deficient mice. *PLoS One* 9: e88563, 2014.

39. **Longenecker CT, Funderburg NT, Jiang Y, Debanne S, Storer N, Labbato DE, Lederman MM, and McComsey GA**. Markers of inflammation and CD8 T-cell activation, but not monocyte activation, are associated with subclinical carotid artery disease in HIV-infected individuals. *HIV Med* 14: 385-390, 2013.

40. **Lynch DH**. The promise of 4-1BB (CD137)-mediated immunomodulation and the immunotherapy of cancer. *Immunol Rev* 222: 277-286, 2008.

41. **Menoret A, Buturla JA, Xu MM, Svedova J, Kumar S, Rathinam VAK, and Vella AT**. T cell-directed IL-17 production by lung granular gammadelta T cells is coordinated by a novel IL-2 and IL-1beta circuit. *Mucosal Immunol* 11: 1398-1407, 2018.

42. **Michel J, and Schwarz H**. Expression of soluble CD137 correlates with activation-induced cell death of lymphocytes. *Cytokine* 12: 742-746, 2000.

43. **Murphy PA, Butty VL, Boutz PL, Begum S, Kimble AL, Sharp PA, Burge CB, and Hynes RO**. Alternative RNA splicing in the endothelium mediated in part by Rbfox2 regulates the arterial response to low flow. *Elife* 7: 2018.

44. **Murphy PA, and Hynes RO**. Alternative splicing of endothelial fibronectin is induced by disturbed hemodynamics and protects against hemorrhage of the vessel wall. *Arterioscler Thromb Vasc Biol* 34: 2042-2050, 2014.

45. **Nam D, Ni CW, Rezvan A, Suo J, Budzyn K, Llanos A, Harrison DG, Giddens DP, and Jo H**. A model of disturbed flow-induced atherosclerosis in mouse carotid artery by partial ligation and a simple method of RNA isolation from carotid endothelium. *J Vis Exp* 2010.

46. **Ng CT, Fong LY, Sulaiman MR, Moklas MA, Yong YK, Hakim MN, and Ahmad Z**. Interferon-Gamma Increases Endothelial Permeability by Causing Activation of p38 MAP Kinase and Actin Cytoskeleton Alteration. *J Interferon Cytokine Res* 35: 513-522, 2015.

47. **Oksenberg JR, Stavri GT, Jeong MC, Garovoy N, Salisbury JR, and Erusalimsky JD**. Analysis of the T-cell receptor repertoire in human atherosclerosis. *Cardiovasc Res* 36: 256-267, 1997.

48. **Olofsson PS, Soderstrom LA, Wagsater D, Sheikine Y, Ocaya P, Lang F, Rabu C, Chen L, Rudling M, Aukrust P, Hedin U, Paulsson-Berne G, Sirsjo A, and Hansson GK**. CD137 is expressed in human atherosclerosis and promotes development of plaque inflammation in hypercholesterolemic mice. *Circulation* 117: 1292-1301, 2008.

49. **Papa A, Danese S, Urgesi R, Grillo A, Guglielmo S, Roberto I, Bonizzi M, Guidi L, De Vitis I, Santoliquido A, Fedeli G, Gasbarrini G, and Gasbarrini A**. Early atherosclerosis in patients with inflammatory bowel disease. *Eur Rev Med Pharmacol Sci* 10: 7-11, 2006.

50. **Qualai J, Li LX, Cantero J, Tarrats A, Fernandez MA, Sumoy L, Rodolosse A, McSorley SJ, and Genesca M**. Expression of CD11c Is Associated with Unconventional Activated T Cell Subsets with High Migratory Potential. *PLoS One* 11: e0154253, 2016.

51. **Ranjbaran H, Sokol SI, Gallo A, Eid RE, Iakimov AO, D'Alessio A, Kapoor JR, Akhtar S, Howes CJ, Aslan M, Pfau S, Pober JS, and Tellides G**. An inflammatory pathway of IFN-gamma production in coronary atherosclerosis. *J Immunol* 178: 592-604, 2007.

52. **Ridker PM, Cannon CP, Morrow D, Rifai N, Rose LM, McCabe CH, Pfeffer MA, Braunwald E, Pravastatin or Atorvastatin E, and Infection Therapy-Thrombolysis in Myocardial Infarction I**. C-reactive protein levels and outcomes after statin therapy. *N Engl J Med* 352: 20-28, 2005.

53. **Ridker PM, Everett BM, Thuren T, MacFadyen JG, Chang WH, Ballantyne C, Fonseca F, Nicolau J, Koenig W, Anker SD, Kastelein JJP, Cornel JH, Pais P, Pella D, Genest J, Cifkova R, Lorenzatti A,**

Forster T, Kobalava Z, Vida-Simiti L, Flather M, Shimokawa H, Ogawa H, Dellborg M, Rossi PRF, Troquay RPT, Libby P, Glynn RJ, and Group CT. Antiinflammatory Therapy with Canakinumab for Atherosclerotic Disease. *N Engl J Med* 377: 1119-1131, 2017.

54. **Robertson AK, and Hansson GK**. T cells in atherogenesis: for better or for worse? *Arterioscler Thromb Vasc Biol* 26: 2421-2432, 2006.

55. **Roche-Molina M, Sanz-Rosa D, Cruz FM, Garcia-Prieto J, Lopez S, Abia R, Muriana FJ, Fuster V, Ibanez B, and Bernal JA**. Induction of sustained hypercholesterolemia by single adeno-associated virus-mediated gene transfer of mutant hPCSK9. *Arterioscler Thromb Vasc Biol* 35: 50-59, 2015.

56. **Ross R**. Atherosclerosis--an inflammatory disease. *N Engl J Med* 340: 115-126, 1999.

57. **Sharief MK**. Heightened intrathecal release of soluble CD137 in patients with multiple sclerosis. *Eur J Neurol* 9: 49-54, 2002.

58. **Sherer Y, and Shoenfeld Y**. Mechanisms of disease: atherosclerosis in autoimmune diseases. *Nat Clin Pract Rheumatol* 2: 99-106, 2006.

59. **Soderstrom LA, Gertow K, Folkersen L, Sabater-Lleal M, Sundman E, Sheikine Y, Goel A, Baldassarre D, Humphries SE, de Faire U, Watkins H, Tremoli E, Veglia F, Hamsten A, Hansson GK, and Olofsson PS**. Human genetic evidence for involvement of CD137 in atherosclerosis. *Mol Med* 20: 456-465, 2014.

60. **Soderstrom LA, Jin H, Caravaca AS, Klement ML, Li Y, Gistera A, Hedin U, Maegdefessel L, Hansson GK, and Olofsson PS**. Increased Carotid Artery Lesion Inflammation Upon Treatment With the CD137 Agonistic Antibody 2A. *Circ J* 81: 1945-1952, 2017.

61. **Tse K, Tse H, Sidney J, Sette A, and Ley K**. T cells in atherosclerosis. *Int Immunol* 25: 615-622, 2013.

62. **Tsurutani N, Mittal P, St Rose MC, Ngoi SM, Svedova J, Menoret A, Treadway FB, Laubenbacher R, Suarez-Ramirez JE, Cauley LS, Adler AJ, and Vella AT**. Costimulation Endows Immunotherapeutic CD8 T Cells with IL-36 Responsiveness during Aerobic Glycolysis. *J Immunol* 196: 124-134, 2016.

63. **van de Berg PJ, van Stijn A, Ten Berge IJ, and van Lier RA**. A fingerprint left by cytomegalovirus infection in the human T cell compartment. *J Clin Virol* 41: 213-217, 2008.

64. **van Dijk RA, Duinisveld AJ, Schaapherder AF, Mulder-Stapel A, Hamming JF, Kuiper J, de Boer OJ, van der Wal AC, Kolodgie FD, Virmani R, and Lindeman JH**. A change in inflammatory footprint precedes plaque instability: a systematic evaluation of cellular aspects of the adaptive immune response in human atherosclerosis. *J Am Heart Assoc* 4: 2015.

65. **Vinay DS, Kim CH, Choi BK, and Kwon BS**. Origins and functional basis of regulatory CD11c+CD8+ T cells. *Eur J Immunol* 39: 1552-1563, 2009.

66. **Vozenilek AE, Blackburn CMR, Schilke RM, Chandran S, Castore R, Klein RL, and Woolard MD**. AAV8-mediated overexpression of mPCSK9 in liver differs between male and female mice. *Atherosclerosis* 278: 66-72, 2018.

67. **Weinstein AM, Giraldo NA, Petitprez F, Julie C, Lacroix L, Peschaud F, Emile JF, Marisa L, Fridman WH, Storkus WJ, and Sautes-Fridman C**. Association of IL-36gamma with tertiary lymphoid structures and inflammatory immune infiltrates in human colorectal cancer. *Cancer Immunol Immunother* 2018.

68. **Wen T, Bukczynski J, and Watts TH**. 4-1BB ligand-mediated costimulation of human T cells induces CD4 and CD8 T cell expansion, cytokine production, and the development of cytolytic effector function. *J Immunol* 168: 4897-4906, 2002.

69. **Wilcox RA, Chapoval AI, Gorski KS, Otsuji M, Shin T, Flies DB, Tamada K, Mittler RS, Tsuchiya H, Pardoll DM, and Chen L**. Cutting edge: Expression of functional CD137 receptor by dendritic cells. *J Immunol* 168: 4262-4267, 2002.

70. **Wilcox RA, Tamada K, Strome SE, and Chen L**. Signaling through NK cell-associated CD137 promotes both helper function for CD8+ cytolytic T cells and responsiveness to IL-2 but not cytolytic activity. *J Immunol* 169: 4230-4236, 2002.

71. **Winkels H, Ehinger E, Vassallo M, Buscher K, Dinh HQ, Kobiyama K, Hamers AAJ, Cochain C, Vafadarnejad E, Saliba AE, Zernecke A, Pramod AB, Ghosh AK, Anto Michel N, Hoppe N, Hilgendorf I, Zirlik A, Hedrick CC, Ley K, and Wolf D**. Atlas of the Immune Cell Repertoire in Mouse Atherosclerosis Defined by Single-Cell RNA-Sequencing and Mass Cytometry. *Circ Res* 122: 1675-1688, 2018.

72. **Wolfl M, Kuball J, Ho WY, Nguyen H, Manley TJ, Bleakley M, and Greenberg PD**. Activation-induced expression of CD137 permits detection, isolation, and expansion of the full repertoire of CD8+ T cells responding to antigen without requiring knowledge of epitope specificities. *Blood* 110: 201-210, 2007.

73. **Yan J, Gong J, Liu P, Wang C, and Chen G**. Positive correlation between CD137 expression and complex stenosis morphology in patients with acute coronary syndromes. *Clin Chim Acta* 412: 993-998, 2011.

74. **Yan J, Wang C, Chen R, and Yang H**. Clinical implications of elevated serum soluble CD137 levels in patients with acute coronary syndrome. *Clinics (Sao Paulo)* 68: 193-198, 2013.

Figure 1. PCAL induces LDF-dependent formation of atherosclerotic plaque. **A,** WT mice were injected with AAV-mPCSK9 and placed on HFD. PCAL was performed within 1 wk, introducing LDF within the left carotid and maintaining physiologic laminar flow patterns within the contralateral right. Vessels were harvested 3 wks after ligation. **B**, AAV-mPCSK9 injection and HFD feeding of WT mice induces hyperlipidemia with cholesterol in mg/dL 5-fold higher than mice fed normal chow: mean 537 mg/dL (SD 191) vs 102mg/dL (SD 33). ****P<0.0001 by 2-group t-test, n=6-10 mice/group. **C**, Carotid vessels 3 wks after PCAL showing LDF-mediated atherosclerotic plaque development. Unstained carotid vessels (white scale bar: 1mm) and cross-sectional histopathology of indicated carotid vessels stained with Oil Red O (black scale bar: 50μm).

Figure 2. CD137 costimulation increases recruitment of activated effector CD8 T cells into LDF foci. **A,** Hyperlipidemic CD45.2 WT mice received adoptive transfer of CD45.1 Ova-specific splenocytes 2 wks after PCAL and were immunized with SIINFEKL + rat IgG control or agonist anti-CD137 mAb. **B**, *in vivo* CD137 costimulation induces an activated effector population that is resident in spleen and circulates in blood 4 dpi. Splenocytes and blood cells were stimulated *in vitro* with Media or PMA + ionomycin. *P=0.02, **P=0.009, ***P=0.0004, ****P<0.0001 by paired t-test and $^{\#\#\#}$P<0.0007 by 2-group t-test, n=6-8 mice/group. **C**, Gating Strategy for identifying T cells from PBS-flushed vessels by flow cytometry. CD45.1 indicates transferred population, CD45.2 indicates an endogenous population and Ova-specificity through TCR expression of Vα2β5. Gating scheme is enlarged in Supplemental Figure S1C with isotype stains used to establish gates. **D**, Percentage (gated on viable cells) and total cell count of transferred CD8 T cells isolated from PBS-flushed contralateral control vs. ligated carotids 4 dpi. *P≤0.03, **P=0.004, ***P=0.0002 by 2-group t-test, n=5-6 mice/group. **E**, Percentage of infiltrated transferred CD8 T cells isolated from PBS-flushed Aortic Arch. Data shown is one experiment representative of two experimental replicates. ***P=0.0004 by 2-group t-test n=6-8 mice/group.

Figure 3. CD137 costimulation instigates luminal infiltration of activated effector CD8 T cells. **A.** Hyperlipidemic CD45.2 WT mice received adoptive transfer of CD45.1 Ova-specific splenocytes 2 wks after PCAL and were immunized with SIINFEKL + rat IgG control or agonist anti-CD137 mAb. **B**, Confocal microscopy of ligated carotid vessels 4 dpi with either control IgG treatment or CD137 costimulation stained for ECs (CD31, green), Ova-specific transferred CD8 T cells (CD45.1, red), and DAPI (blue). White squares demarcate magnified images below and arrows indicate infiltrating effector CD8 T cells. (Scale bar top: 50μm top; bottom: 20μm). Intima (I), medial (M), and adventitial (A) layers of the developing plaque are indicated by dashed lines. **C**, Total count of transferred CD8 T cells per carotid vessel cross-section (left) and localization of cells either within intima (top) or at the lumen surface (bottom) in PCAL-carotid cross-sections of mice that received transfer of CD45.1 WT Ova-specific CD8 T cells and immunization with SIINFEKL + rat IgG control or agonist anti-CD137 mAb. Each dot is a carotid cross-section from an individual biologic replicate. ns P=0.09, **P<0.006 by 2-group t-test n=5 mice/group. Data shown is from one experiment representative of two experimental replicates.

Figure 4. Infiltrated T cells have innate-like inflammatory potential. **A,** Hyperlipidemic CD45.2 WT mice received adoptive transfer of CD45.1 Ova-specific splenocytes 2 wks after PCAL and were immunized with SIINFEKL and agonist anti-CD137 mAb. Vessels were harvested 4 dpi. **B,** 4 dpi with SIINFEKL and agonist anti-CD137 mAb, splenocytes have a robust innate-like response to the cytokine combination of IL-2 + IL-36. Cells were stimulated *in vitro* and secreted IFNγ was measured by ELISA analysis of supernatant. ns P>0.1, **P<0.03 by series of paired t-tests, n=5-8/group. **C,** This innate-like secretion was also seen in cells isolated from the Abdominal Aorta, a physiologic site of LDF at intercostal branch points, but not in cells isolated

from the linear carotid, a vessel subjected to laminar high flow (right panel). ns P=0.2, *P=0.015 by paired t-test, n=2-8 mice/group. **D,** Cells isolated from PCAL-ligated carotids have innate-like responses to cytokines (IL-2 + IL-36) and also secrete IFNγ in response to PMA + ionomycin as measured by ELISA. *P<0.02 by paired t-tests, n=6 mice/group.

Figure 5. T cell CD137 expression is critical for infiltration of effector CD8 T cells into LDF foci. **A**, Experimental setup for adoptive transfer of CD45.1 Ova-specific CD8 T cells that are either WT or $CD137^{-/-}$ into normolipidemic CD45.2 WT mice immunized with SIINFEKL and agonist anti-CD137 mAb. Vessels were harvested 4 dpi. **B,** Percentage (gated on viable cells) of Ova-specific transferred CD8 T cells within physiologic areas LDF (Aortic Arch) and high laminar flow (Linear carotid). Data is pooled from 2 experiments, 2-3 mice/group/experiment. ns P=0.3, **P=0.004 by 2-group t-test, n=5/group. **C,** Cell counts of T cells isolated from the Aortic Arch and Linear Carotid 4 dpi. Only the population of Transferred CD8 T cells achieved statistical significance. Population of "Endogenous T cells" is inclusive of endogenous CD8 T cells that are $V\alpha2^{+}\beta5^{+}$ (and thus likely Ova-specific) and non-Vα2β5, as well as endogenous CD4 T cells. For cells isolated from Aortic Arch: ns P=0.5 (Endogenous T cells), *P =0.01 (Transferred CD8 T cells), cells isolated from the Linear Carotid: ns P>0.1 (Transferred and Endogenous CD8 T cells) via Mann-Whitney test. Data is pooled from 2 experiments, 2-3 mice/group/experiment, n=5 mice/group.

Figure 6. Infiltration of CD137 costimulated effector CD8 T cells is persistent within LDF foci. **A,** Experimental setup for mixed adoptive transfer of WT (CD45.1) and $CD137^{-/-}$ (Het CD45.1/2) Ova-specific CD8 T cells. Total number of transferred cells is kept consistent throughout all adoptive transfer experiments. **B,** Normolipidemic mice were harvested 5 and 11 dpi with cognate SIINFEKL and agonist anti-CD137 mAb. Percentage (gated on viable cells) of each transferred population isolated from the Aortic Arch; ns P>0.12 by unpaired 2-tailed Student's t-test, n=5 mice/timepoint. **C,** Count of transferred CD8 T cells per spleen and per 400 µL blood decreases dramatically from 5 to 11 dpi (*P<0.03, *P <0.01), while infiltration of transferred WT Ova-specific CD8 T cells within the aortic arch does not (ns P≥0.3). Significance determined by 2-group t-test, n=5 mice/timepoint. **D,** Percentage (gated on viable cells) of endogenous CD8 populations isolated from the Aortic arch. **** P< 0.0001 by 2-group t-test n=5 mice/timepoint. **E,** Hyperlipidemic, PCAL mice (AAV-mPCSK9 mice on HFD as in Figure 2A) received mixed transfer of WT and $CD137^{-/-}$ Ova-specific CD8 T cells. Mice were harvested 17 dpi and the percentage of each indicated population isolated from either Ligated LDF carotids or the contralateral control right carotids are shown. ns P>0.1 ****P<0.0001 via paired t-test, n=7 mice/group.

Figure 7. Infiltration of effector CD8 T cells promotes a diverse pro-inflammatory infiltrate within nascent atherogenic foci. **A**, Hyperlipidemic mice received transfer of WT or $CD137^{-/-}$ Ova-specific CD8 T cells and were immunized with SIINFEKL and agonist anti-CD137 mAb. 30 dpi, aortic arches were analyzed by flow cytometry for infiltration of transferred CD8 T cells. **B,** Percentage (gated on viable cells) and cell count of transferred CD8 per vessel are shown. ns P>0.2, **P<0.004 by 2-group t-test. n=6-7 mice/group. **C**, Immunohistofluoresence of the branch point of the right subclavian artery from the brachiocephalic artery 30 dpi shows intimal persistence of transferred CD8 T cells (CD45.1 in red) within atherogenic foci.

Figure 8. Infiltration of effector CD8 T cells promotes a diverse pro-inflammatory infiltrate within nascent atherogenic foci. **A**, Hyperlipidemic mice received transfer of WT or $CD137^{-/-}$ Ova-specific CD8 T cells and were immunized with SIINFEKL and agonist anti-CD137 mAb. 30 dpi,

aortic arches were analyzed by flow cytometry for infiltration of transferred CD8 T cells. **B,** Cells isolated from aortic arch were stimulated for 40 h with PMA + ionomycin and 5 h with Brefeldin A. Intracellular IFNγ analyzed through flow cytometry (gated on total events) and T cell distribution of WT transfer IFNγ^{+} response (gated on IFNγ^{+} cells). *P=0.01 by 2-group t-test. **C**, Infiltration of endogenous CD8 T cells that do not express the Ova-specific TCR (Vα2Vβ5) have increased infiltration of the aortic arch 30 dpi when the atherogenic foci is first seeded with WT effector CD8 T cells. Infiltration of endogenous, CD137-sufficient Ova-specific CD8 T cells was not statistically significant. ns P=0.3, ***P=0.0006 by 2-group t-test. **D**, CD11c MFI expression from indicated T cell subsets isolated from aortic arch of mice that received WT Ova-specific CD8 T cells. ns P=0.8, ***P=0.0005, ****P<0.0001 via paired t-tests. **E**, Intracellular cytokine staining after stimulation with Media, Cytokines (IL-2 + IL-36), or SIINFEKL gated on total events on cells isolated from the aortic arch of mice that received WT or CD137$^{-/-}$ transfer of CD8 T cells. ns P>0.1, *P=0.01, **P=0.006 by paired t-test. **F,** Cells isolated from the Aortic Arch 30 dpi secrete IFNγ in response to the cytokine combination of IL-2 + IL-36, but not SIINFEKL cognate antigen restimulation. *P=0.03, ns P>0.2 via Wilcoxon matched-pairs test, $^{\#\#}$P=0.001 via Mann-Whitney test, n=6-7 mice/group for all experiments in Figure 8.

Figure 9. Proposed model for how CD137 costimulation promotes the seeding of activated effector CD8 T cells into nascent atherogenic foci. **A**, Under conditions of homeostatic health, naive CD8 T cells do not readily infiltrate the vessel wall, even at sites of LDF-activated endothelium, where adhesion receptors or chemokines are upregulated (red dashed line). **B,** Increased circulation of effector CD8 T cells by CD137 costimulation prompts their infiltration at LDF foci, independent of cognate TCR recognition. **C**, LDF activates intimal cells at atherogenic foci to secrete cytokines, such as IL-36γ, which promote innate-like secretion of IFNγ from infiltrated CD8 T cells. **D,** Pro-inflammatory cytokines produced in (C) further alter the plaque microenvironment, generating an intimal niche (yellow dashed line) that is permissive to infiltration of other CD8 T cells in circulation. **E**, Together, the initial seeding of CD137-stimulated effector CD8 T cells and the subsequent infiltration of other CD8 T cells constitute a plaque with increased inflammatory potential, potentially resulting in accelerated atherosclerotic pathology and vascular events.

Supplemental Figure S1. LDF promotes cellular, atherosclerotic plaque development within 3 wks and CD137 costimulation does not substantially affect CD4 T cell infiltration.
A, Representative, cross-sectional DAPI staining of carotid vessels 3 wks after PCAL procedure. PBS-flushed vessels were collected, sectioned, stained, and imaged at 20x, scale bar: 50μm. Intimal plaque is highlighted with a dashed yellow line. **B,** Hyperlipidemic CD45.2 WT mice received adoptive transfer of CD45.1 Ova-specific splenocytes 2 wks after PCAL and were immunized with SIINFEKL + rat IgG control or agonist anti-CD137 mAb (Figure 2A). 4 dpi, infiltration of CD4 T cells is unaffected by CD137 costimulation. ns P>0.4 by 2-group t-test, n=5 mice/group. **C**, Enlarged gating strategy (Figure 2C) for identifying T cells from PBS-flushed vessels by flow cytometry. CD45.1 indicates transferred population, CD45.2 indicates an endogenous population. Ova-specificity was determined through T cell Receptor expression of Vα2β5. Isotype stains for ***i.*** T cells: CD8 and CD4, ***ii.*** Ova-specific TCRs Vα2 and Vβ5, and ***iii.*** Congenic markers: CD45.1 and CD45.2 are shown in the panel below on both spleen samples (dotted line) and vessel samples (grey) with a representative Ligated LDF vessel sample shown in blue below.

Supplemental Figure S2. Transferred effector CD8 T cell infiltration is not substantially affected by lipid levels. Cholesterol level of mPCSK9-hyperlipidemic mice at harvest (as in Figure 2A) plotted against percentage of transferred CD8 T cells (gated on viable cells) and total

transferred CD8 T cells isolated from the indicated LDF vessel. Linear regression lines graphed, no slopes achieved statistical significance; all P>0.1, n=4-6 mice/group.

Supplemental Figure S3. CD137 costimulation promotes intimal infiltration of effector CD8 T cells. Hyperlipidemic CD45.2 WT mice received adoptive transfer of CD45.1 Ova-specific splenocytes 2 wks after PCAL and were immunized with SIINFEKL + rat IgG control (top panel) or agonist anti-CD137 mAb (bottom panel) as in Figure 2A and 3. PBS-flushed vessels were collected 4 dpi, sectioned, stained, and imaged at 20x. **A,** Quantification of cell infiltration and localization is depicted. Bottom left image depicts localization of lumen (L), intima (I), media (M), and adventitia (A) as defined by non-specific elastin staining. **B,** Bottom panel shows split DAPI channel thresholded between 90-255 to enhance contrast and visibility.

Supplemental Figure S4. LDF mediates an atherogenic foci that is infiltrated by endogenous and infiltrative effector CD8 T cells with innate-like surface markers. **A,** Hyperlipidemic WT CD45.2 mice received transfer of CD45.1 Ova-specific CD8 T cells and were immunized with SIINFEKL and agonist anti-CD137 mAb. viSNE map of PCAL-carotid and contralateral control right carotids vessels revealed two islands of LDF-dominated cells (blue populations) that we then subjected to expression analysis for the panel of metal-conjugated antibodies (Supplemental Table S8). **B,** Expression analysis of LDF Group 1 and Group 2. LDF group 1 is composed primarily of an endogenous (CD45.2) CD11b population while LDF Group 2 is dominated by the transferred, CD137-costimulated effector CD8 population (CD45.2 and CD8) that co-express “innate-like” markers of CD11c and CD161.

Supplemental Figure S5. Atherogenic foci are infiltrated with “innate-like” CD8 T cell phenotypes and in response to LDF, intimal cells upregulate inflammatory cytokines that can elicit innate-like secretion of IFNγ. **A,** PCAL activates vessel intimal cells to expresses IL-1β (IL1B) 48 h after LDF induction. The activating enzyme for IL-36 processing Cathepsin S (CTSS) is also specifically induced by LDF, but outside of IL-36γ (IL36G), no other IL-1 family member was upregulated in response to LDF. ns P>0.6, *P<0.01, **P<0.004, ***P<0.0006 by paired t-test, each dot represents a separate pool of biologic replicates run across 2 lanes. **B,** Secreted IFNγ from *in vitro* stimulation of Ligated-LDF infiltrated cells with cytokines (IL-2 + IL-36) and PMA + ionomycin trends with count of transferred CD8 T cells/vessel. Linear Regression best-fit lines with *P<0.002 for mice with IgG control and indicated P values for CD137-costimulated mice, n=6-7 mice/group. **C,** Ova-specific CD8 T cells were transferred into WT recipient and dual costimulated with agonist anti-CD134 and anti-CD137 mAbs. Splenocytes were isolated 4 dpi and stimulated in vitro with the indicated cytokines for 16 h. Data shown are technical triplicates from a pool of 3 mice, *P<0.02, **P=0.005 by paired t-test.

Supplemental Figure S6. CD137 expression on effector CD8 T cells is necessary for infiltration into surgically-induced and physiologic LDF foci. **A,** PCAL Hyperlipidemic WT mice received WT or $CD137^{-/-}$ Ova-specific CD8 T cells and stimulated with SIINFEKL and agonist anti-CD137 mAb. Infiltration of transferred CD8 T cells was statistically significant in the aortic arch of these mice and borderline significant in ligated-LDF carotid vessels. ns P=0.05, **P=0.004 via Mann-Whitney tests. Aortic Arch n=7-8/group, PCAL-LDF n=5-6/group. **B,** Flow cytometry analysis of $CD8^{+}$ T cells from blood plotted on congenic CD45 markers to identify CD8 T cells as transferred WT (CD45.1), transferred $CD137^{-/-}$ (CD45.1/45.2 Het), and endogenous (CD45.2) as proposed in Figure 6A.

Supplemental Figure S7. CD137 costimulation promotes long-term residence of effector CD8 T cells that have unique innate-like inflammatory potential in atherogenic foci. Hyperlipidemic CD45.2 WT mice received adoptive transfer of either WT or $CD137^{-/-}$ CD45.1 Ova-specific CD8

T cells and immunized with SIINFEKL and agonist anti-CD137 mAb. Spleen, Blood, and vessels were obtained 30 dpi. **A**, Overt expansion of immune cells in response to antigen priming and costimulation is no longer apparent within the spleen or circulating in blood. Total cell counts isolated per spleen are shown. ns P>0.8 by 2-group t-test n=6-7 mice/group. **B**, Cells isolated from the aortic arch have increased secretion of IFNγ upon in vitro stimulation with PMA + ionomycin as evidenced by ELISA. ***P=0.0002 by 2-group t-test, n=6-7 mice/group. **C**, Infiltration of endogenous (CD45.2) CD4 T cells at 30 dpi is unaffected by infiltration of effector CD8 T cells. ns P>0.3 by 2-group t-test, n=6-7 mice/group. **D**, Splenocytes isolated from mice 30 dpi were stimulated in vitro with Media, Cytokines (IL-2 + IL-36) or SIINFEKL peptide. Secretion of IFNγ was assessed by ELISA (left) and intracellular cytokine staining (right). ns P=0.2, *P=0.02, **P=0.002 via paired t-test, n=6-7 mice/group.

Supplemental Table S8. CyTOF Staining Panel. List of heavy metal-conjugated mAbs used in CyTOF studies (Fluidigm, San Francisco, CA).

https://zenodo.org/record/2598759

Figure 1

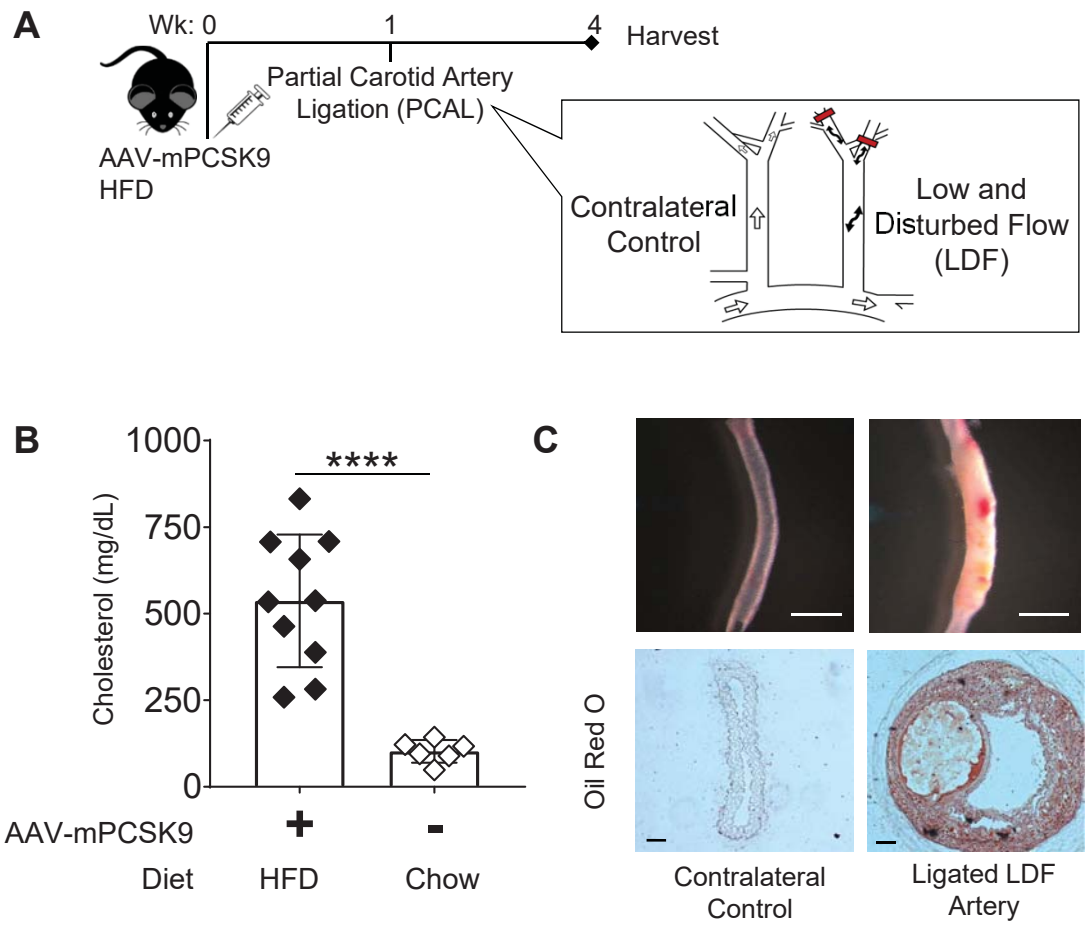

Figure 2

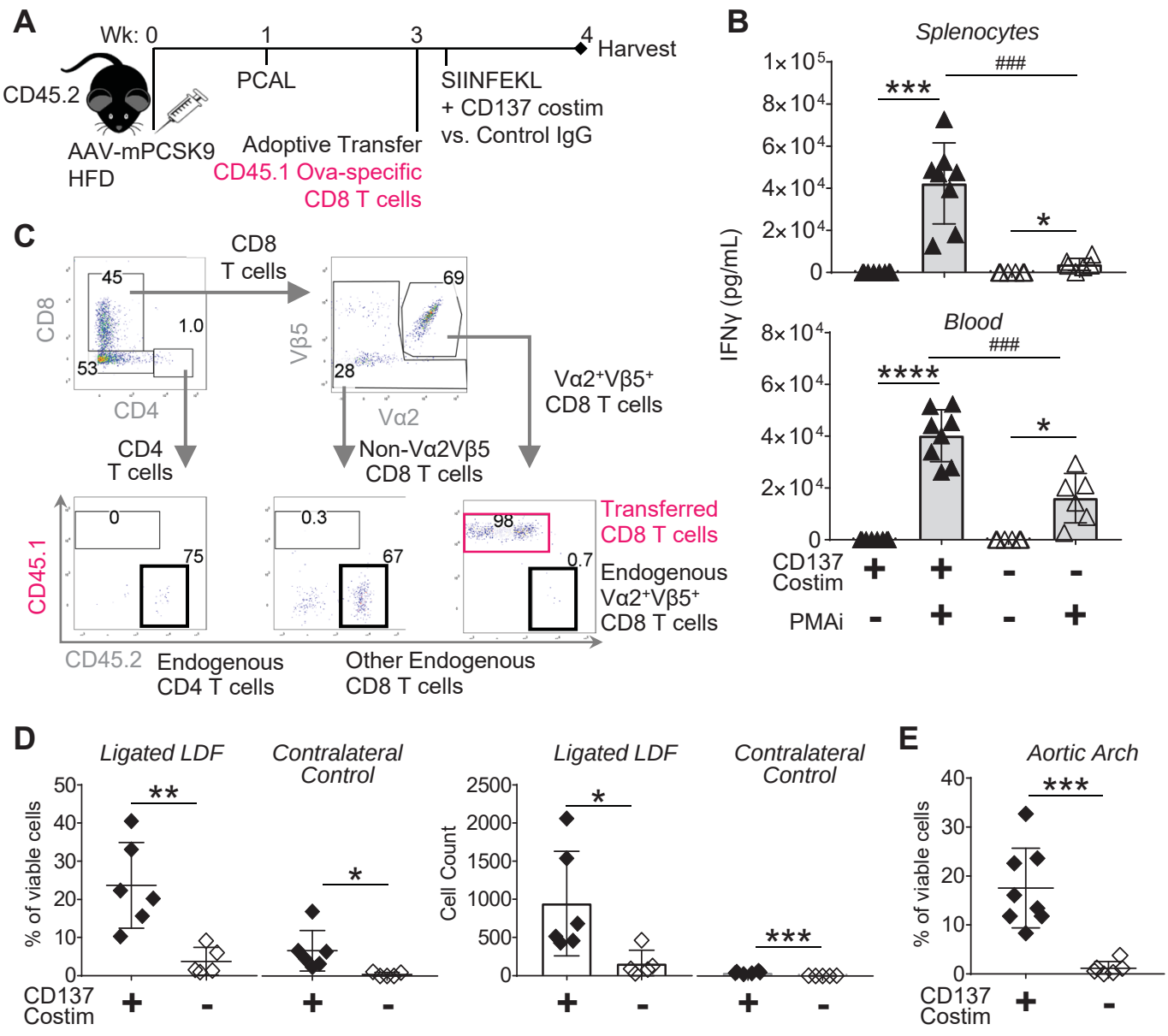

Figure 3

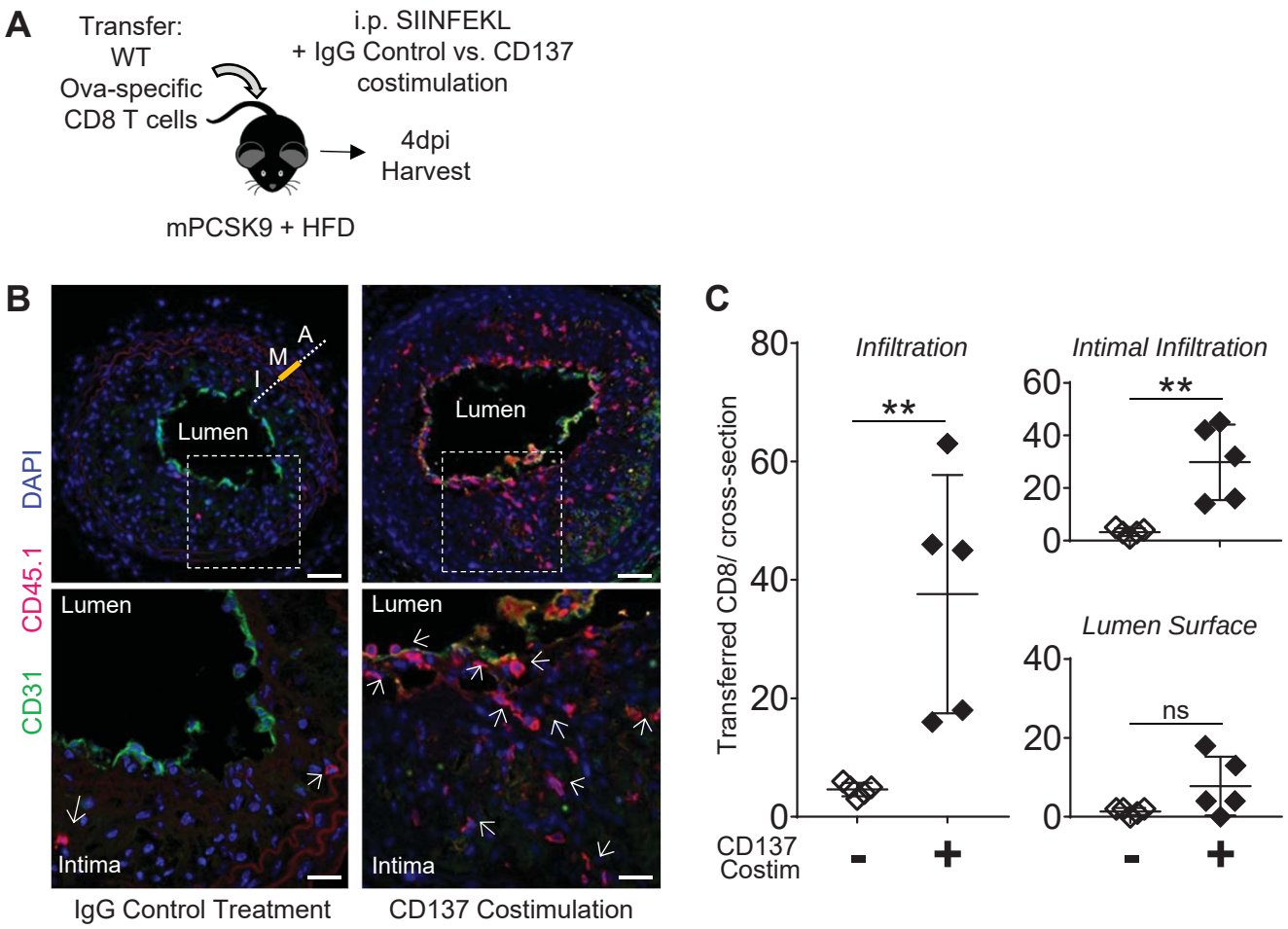

Figure 4

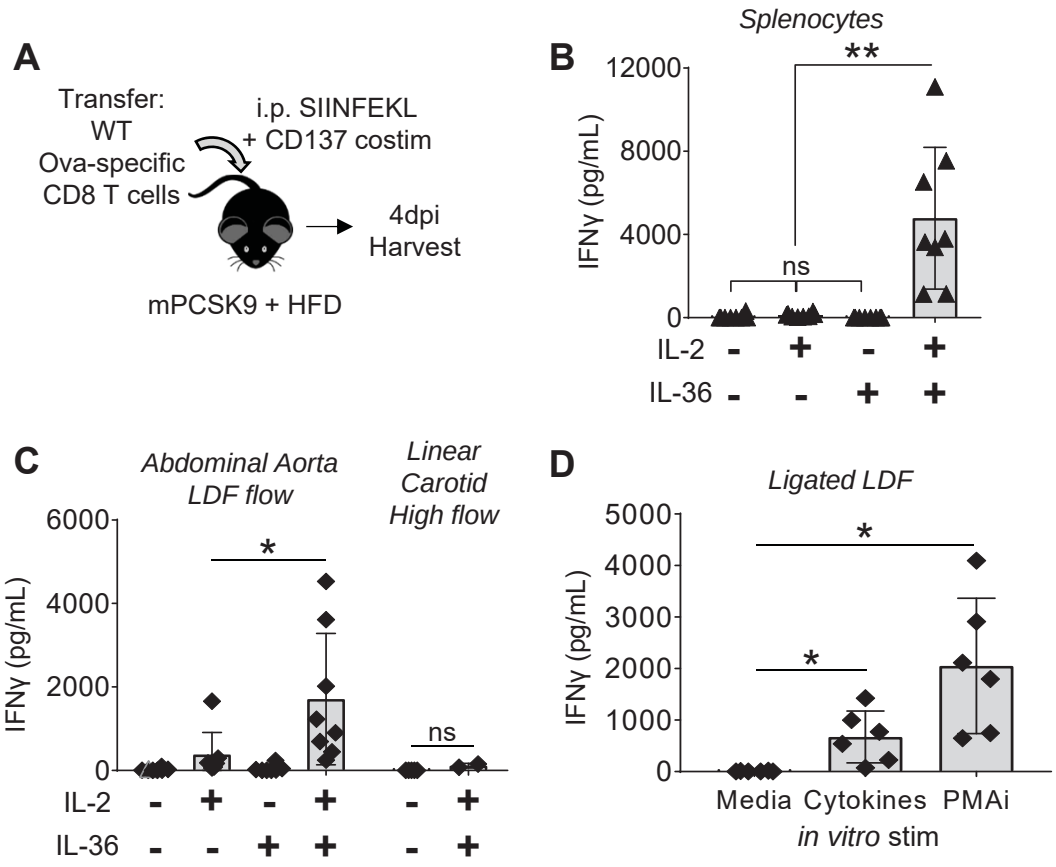

Figure 5

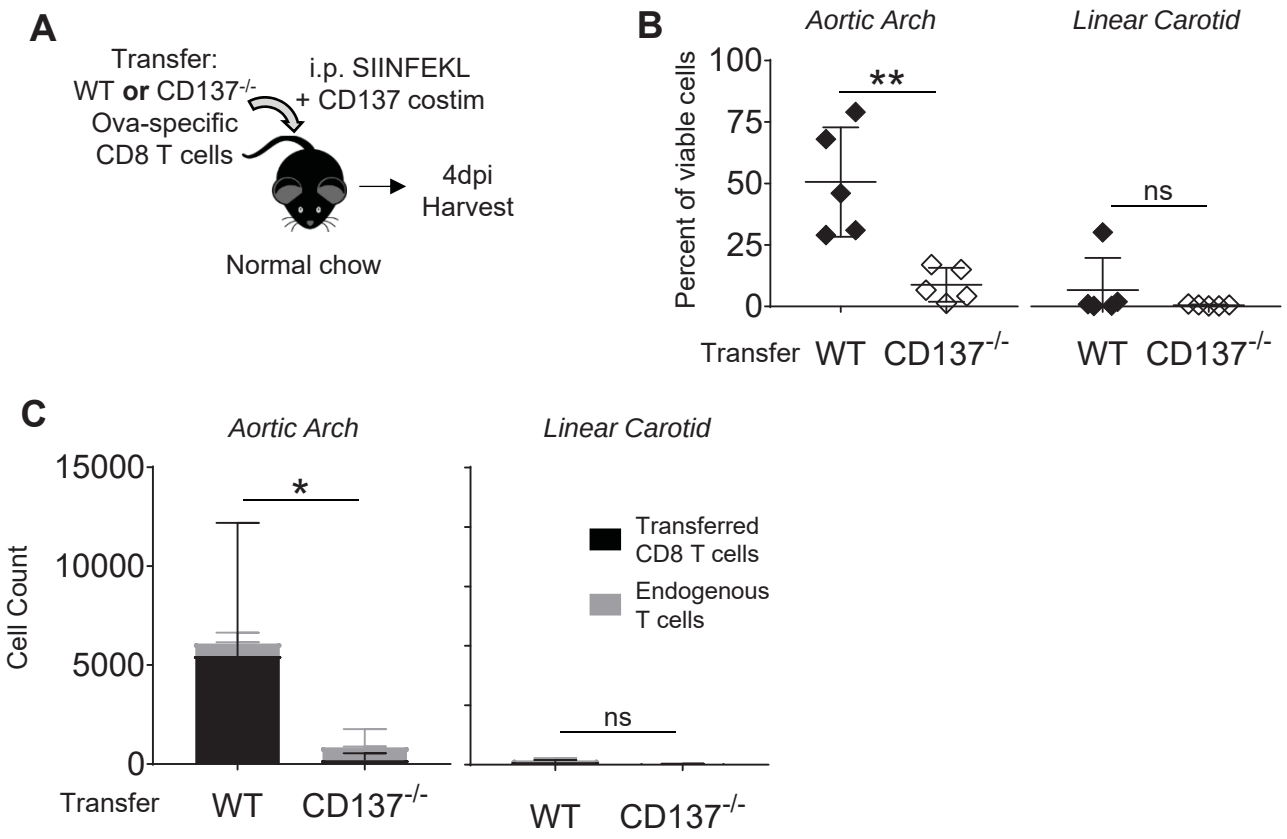

Figure 6

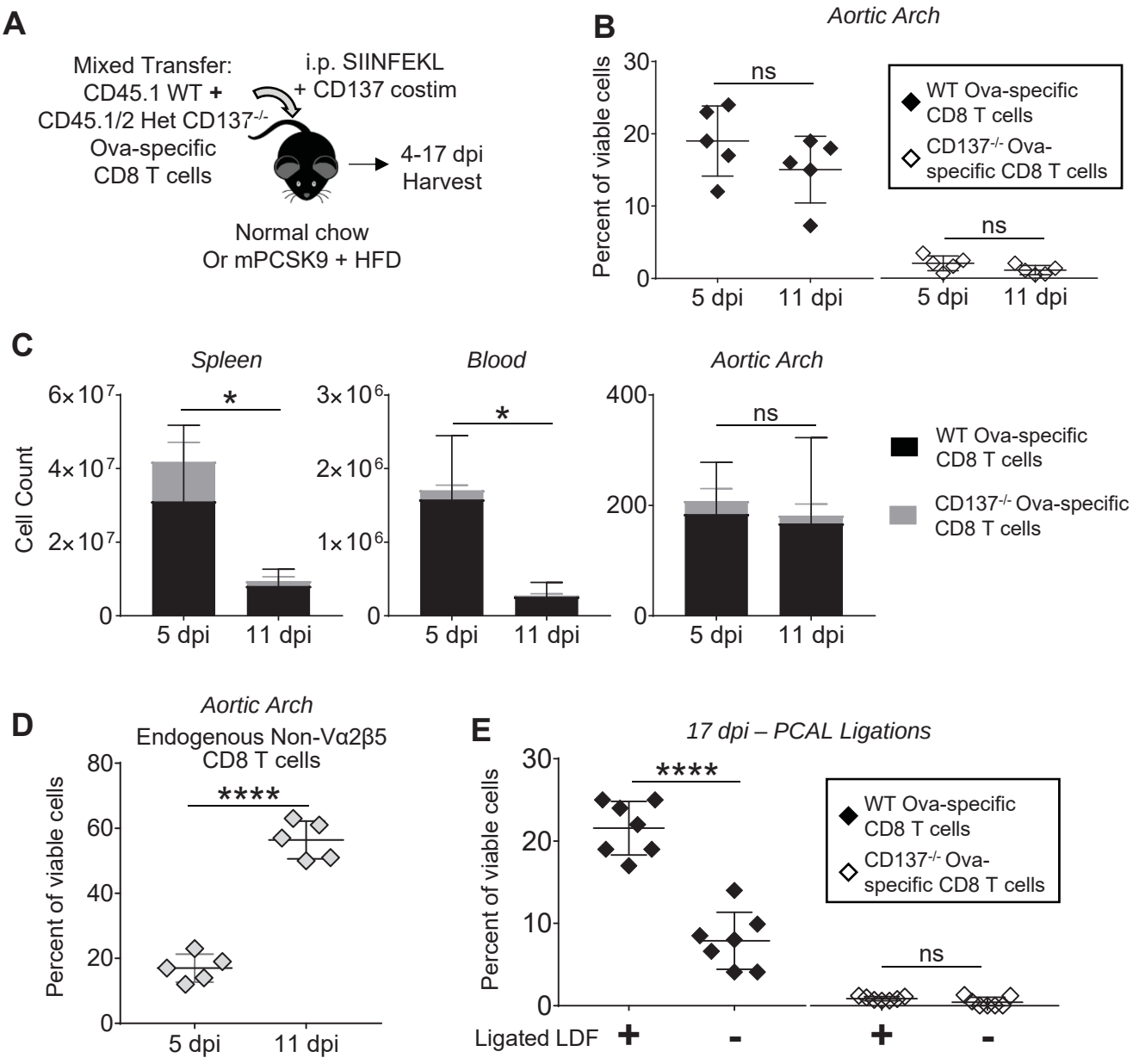

Figure 7

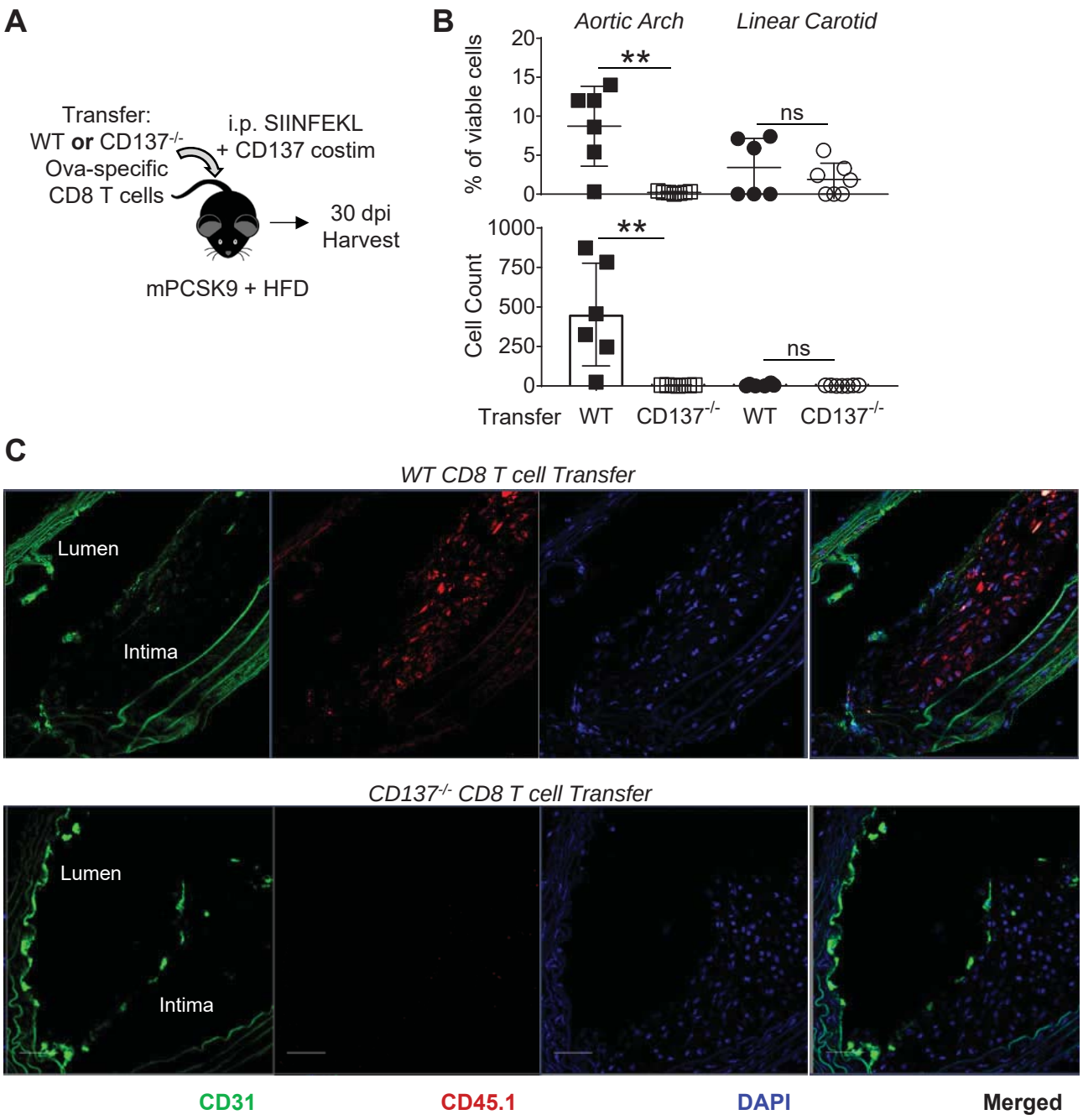

Figure 8

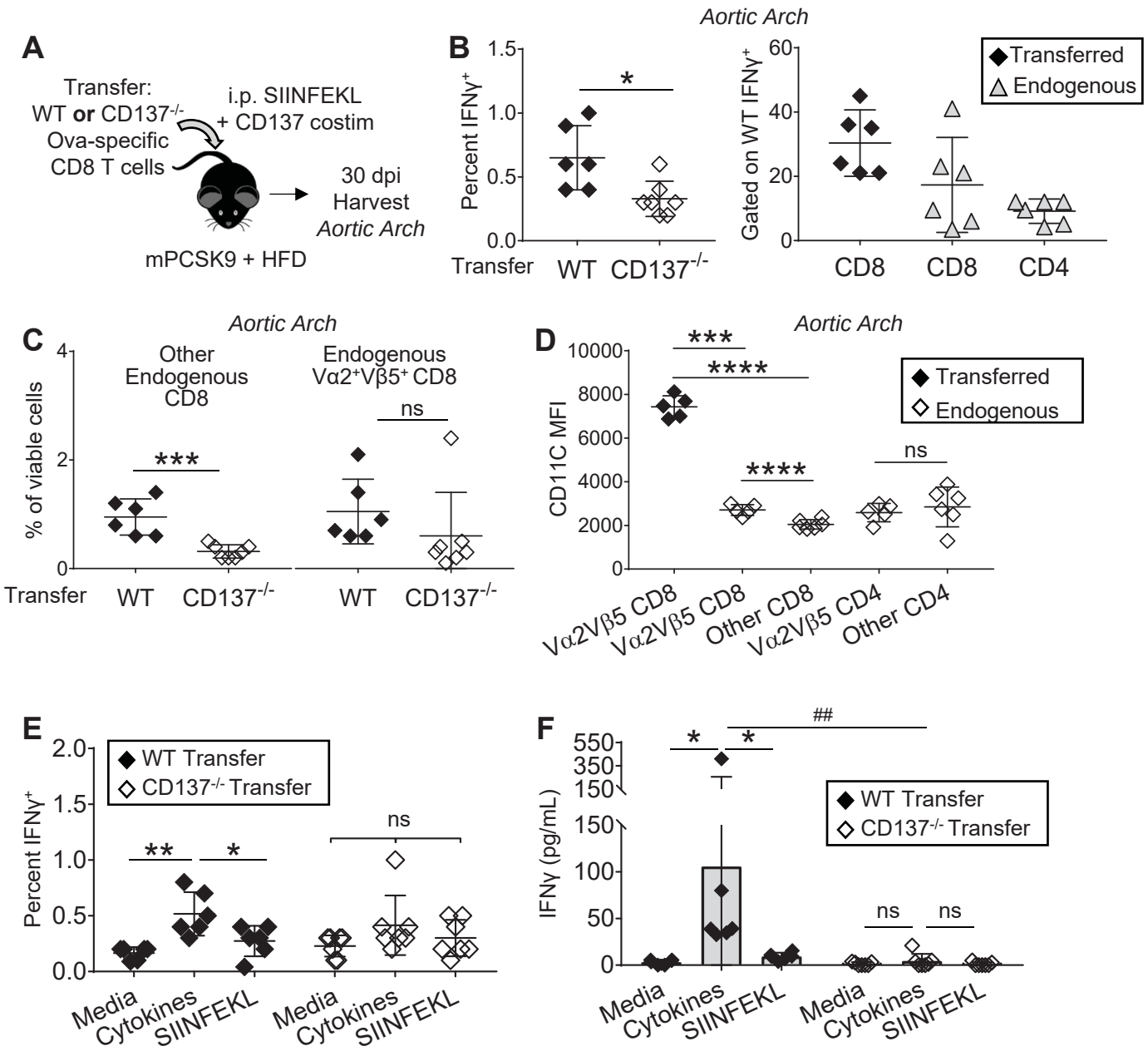

Figure 9